Entry Systems and Technology Division
Ames Research Center

National Aeronautics and
Space Administration

Certification by Analysis of Woven TPS: Fiber- and Weave-Scale Modeling

EDL Summer Seminar

Sergio Fraile Izquierdo, Andrew P. Santos
AMA Inc., Thermal Protection Materials Branch, NASA Ames Research Center, Moffett Field, CA, USA
Lauren J. Abbott
Thermal Protection Materials Branch, NASA Ames Research Center, Moffett Field, CA, USA

July 6, 2023

ANALYTICAL MECHANICS ASSOCIATES

Acknowledgements

Entry Systems Modeling (ESM) Project
TPS Certification by Analysis

Core Team Members

ARC
Justin Haskins
Lauren Abbott
Sergio Fraile Izquierdo
Sander Visser
Andrew Santos
Federico Semeraro
William Tucker
Kevin Wheeler
Vasyl Hafiychuk
Michael von Pohle
Karan Doss

GRC
Trenton Ricks
Brett Bednarcyk
Subodh Mital
Pappu Murthy
Evan Pineda

NASA ARC

Kyle Hendrickson
Magnus Haw
Tane Boghozian
Gurpreet Klar
Don Ellerby
Keith Peterson
Todd White
Jeremy Vander Kam

NASA GRC

Stephanie Vivod
Sadeq Malakooti
Richard Martin

Interns / NSTF / NSTGRO

Will Schill, Caltech
Aaron Allred, CU Boulder
Chloe Zeller, UMN
Michael Olaya, U Mass Lowell
Victoria Arias, UIUC
Joseph Ferguson, Stanford

Woven Thermal Protection Systems (TPS)

Heat Shield for Extreme Entry Environment Technology (HEEET)

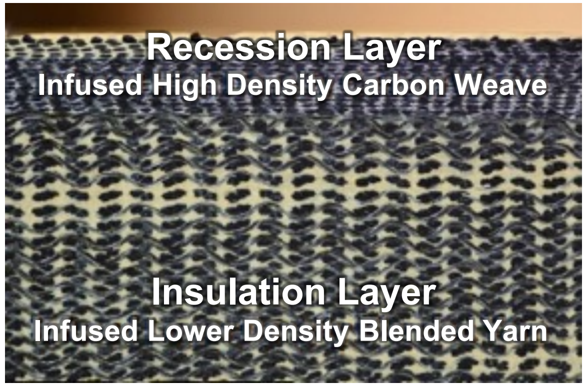

3D Woven Mid-Density Carbon Phenolic (3MDCP)

- ➢ Derived from HEEET insulation layer
- ➢ Mars Sample Return Earth Entry System (MSR-EES)

Adaptable Deployable Entry and Placement Technology (ADEPT)

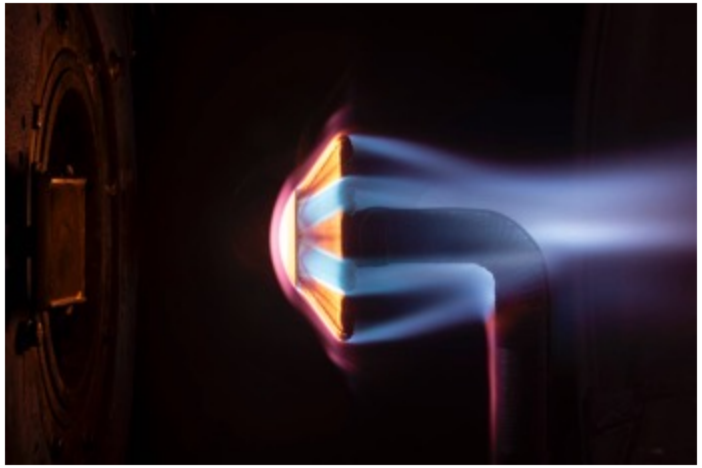

Uninfused Weave

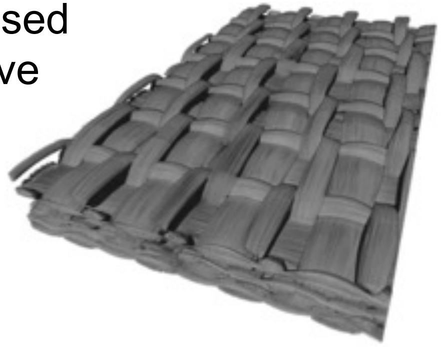

D Ellerby et al, MS&T, 2019 • A Vanaerschot et al, Composite Structures, 2017, 173, 44-52

Certification by Analysis of Woven TPS

Goal: Develop computational tools and techniques to support certification of woven TPS materials

- Identify and characterize material features, defects, and damage
- Determine how these features/defects/damage affect properties, performance, and failure

Weave features or defects

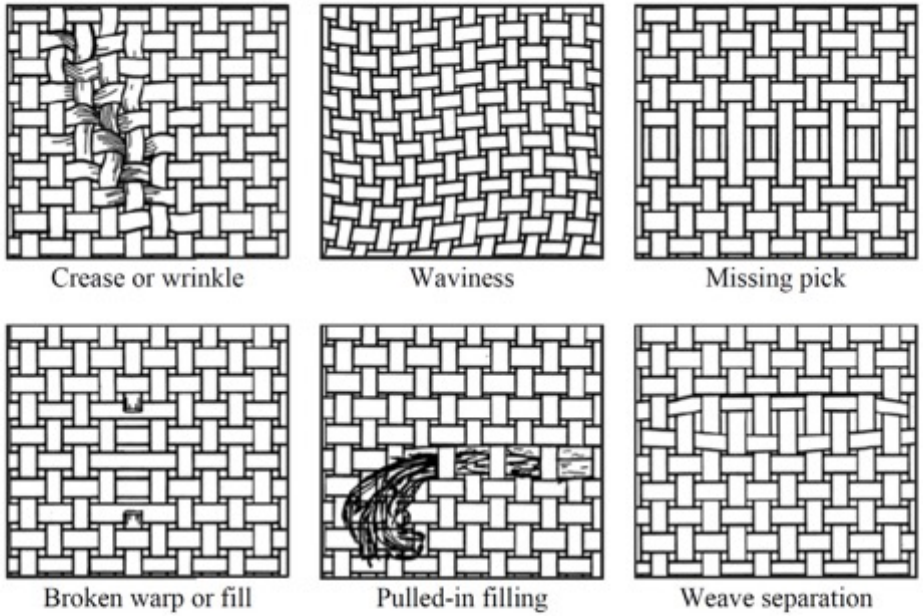

Impact from micrometeoroids and orbital debris (MMOD)

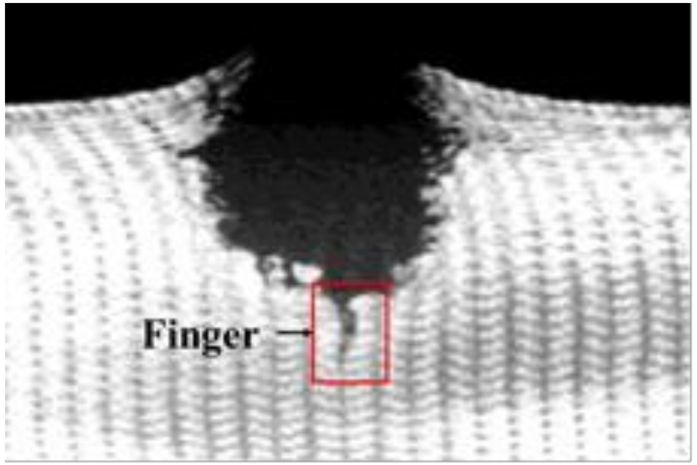

TPS Certification by Analysis Thrusts

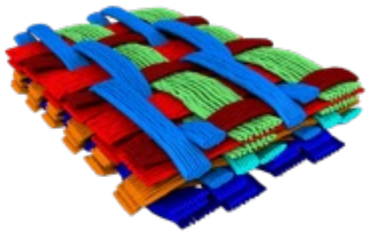

Multiscale Materials Modeling

Ames Research Center

Thermal Protection Materials Branch

Justin Haskins
Lauren Abbott
Andrew Santos
Sergio Fraile Izquierdo

William Tucker
Federico Semeraro
Sander Visser

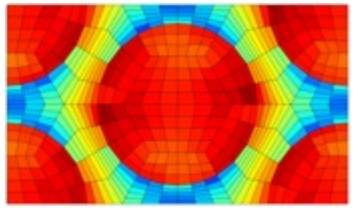

Multiscale Materials Modeling

Glenn Research Center

Multiscale & Multiphysics Modeling Branch

Trenton Ricks
Brett Bednarcyk
Subodh Mital

Pappu Murthy
Evan Pineda

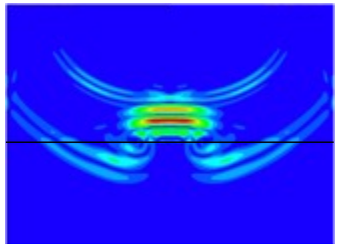

Machine Learning and Nondestructive Evaluation

Ames Research Center

Intelligent Systems Division

Kevin Wheeler
Vasyl Hafiychuk

Michael von Pohle
Karan Doss

TPS Cert Activities: Fault Detection

Computational Nondestructive Evaluation (CNDE)

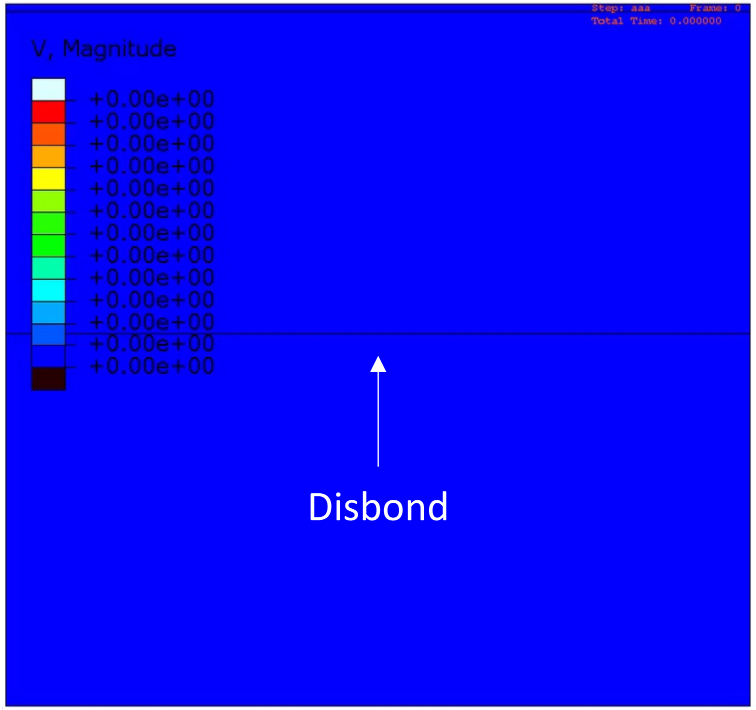

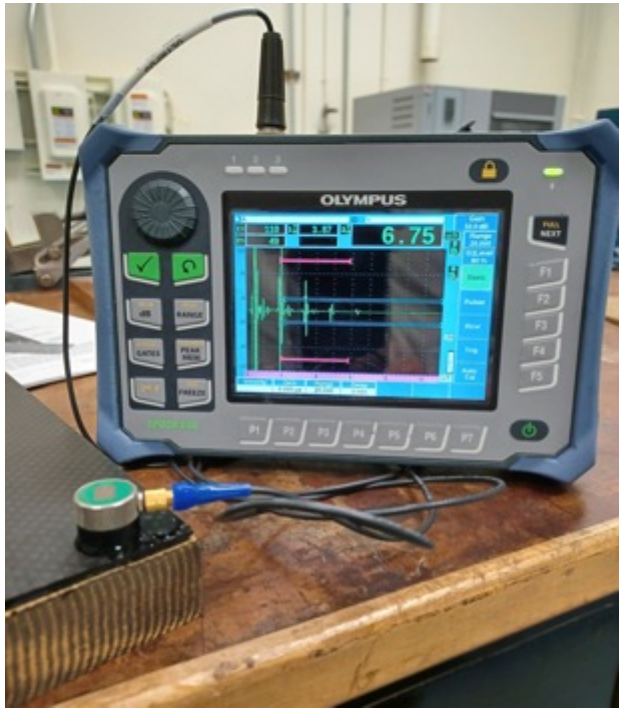

Detection of disbonds by ultrasonic interrogation

POC: Vasyl Hafiychuk (ARC/TI)

Machine Learning

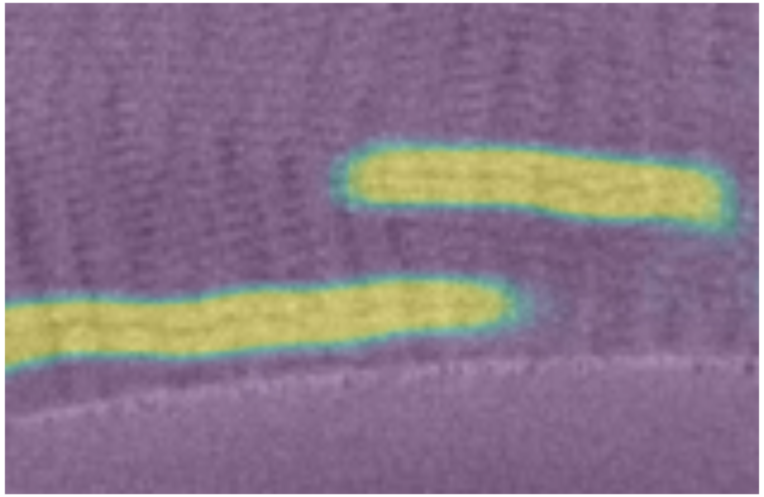

Automated detection of faults in CT scans using deep learning

POC: Michael von Pohle (ARC/TI)

TPS Cert Activities: Damage Simulations

Progressive Damage Simulations

Tensile Shear

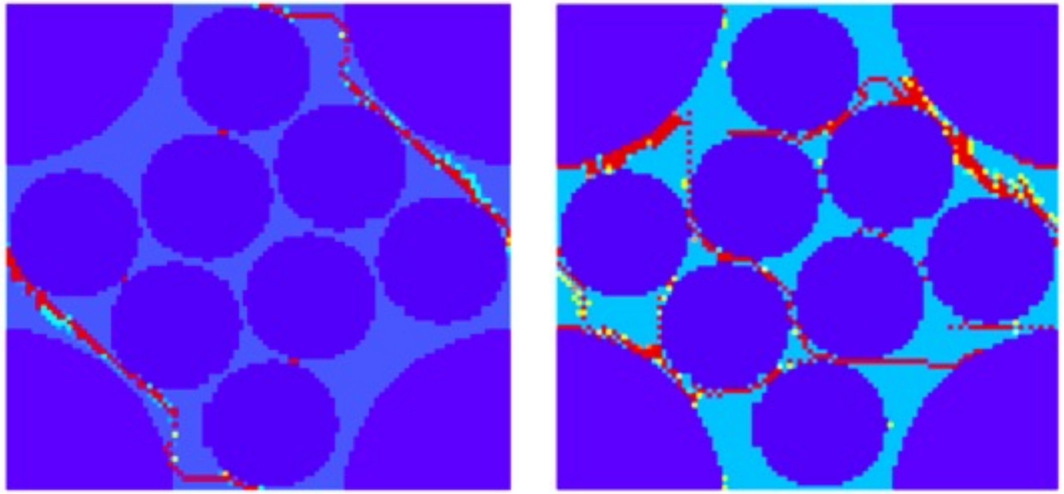

Stress damage in blended yarns using multiscale recursive micromechanics models

POC: Brett Bednarcyk (GRC)

Impact Simulations

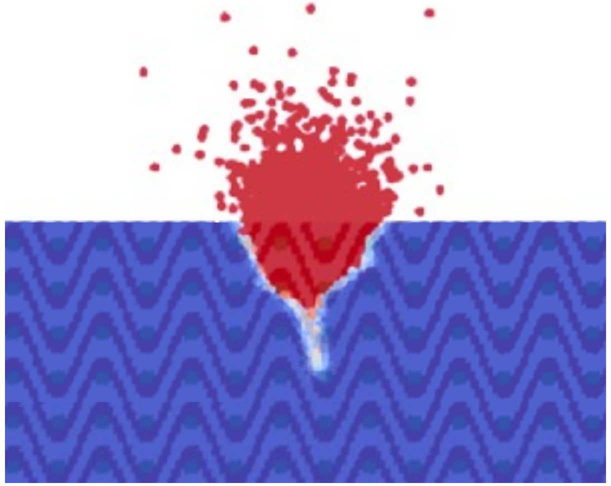

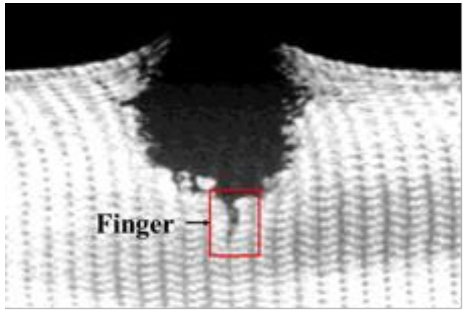

Impact damage using peridynamics simulations with microstructure representation

POC: Justin Haskins (ARC/TSM)

Computational Materials Modeling

Increased Structural Refinement

Particle-based, discrete-element methods (LAMMPS, HYDRA)

Fiber-level resolution

Andrew P. Santos

Porous Microstructure Analysis (PuMA)

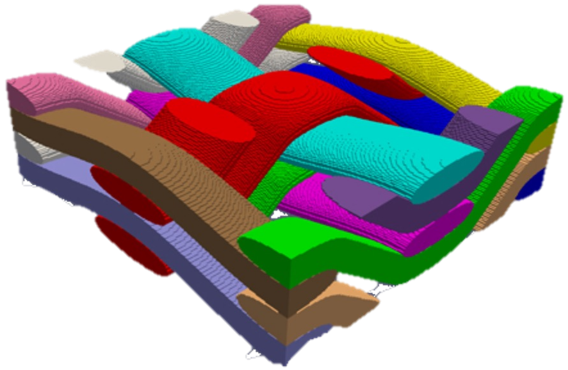

Yarn-level resolution

Sergio Friale Izquierdo

Increased Scale and Analysis

Table of Contents

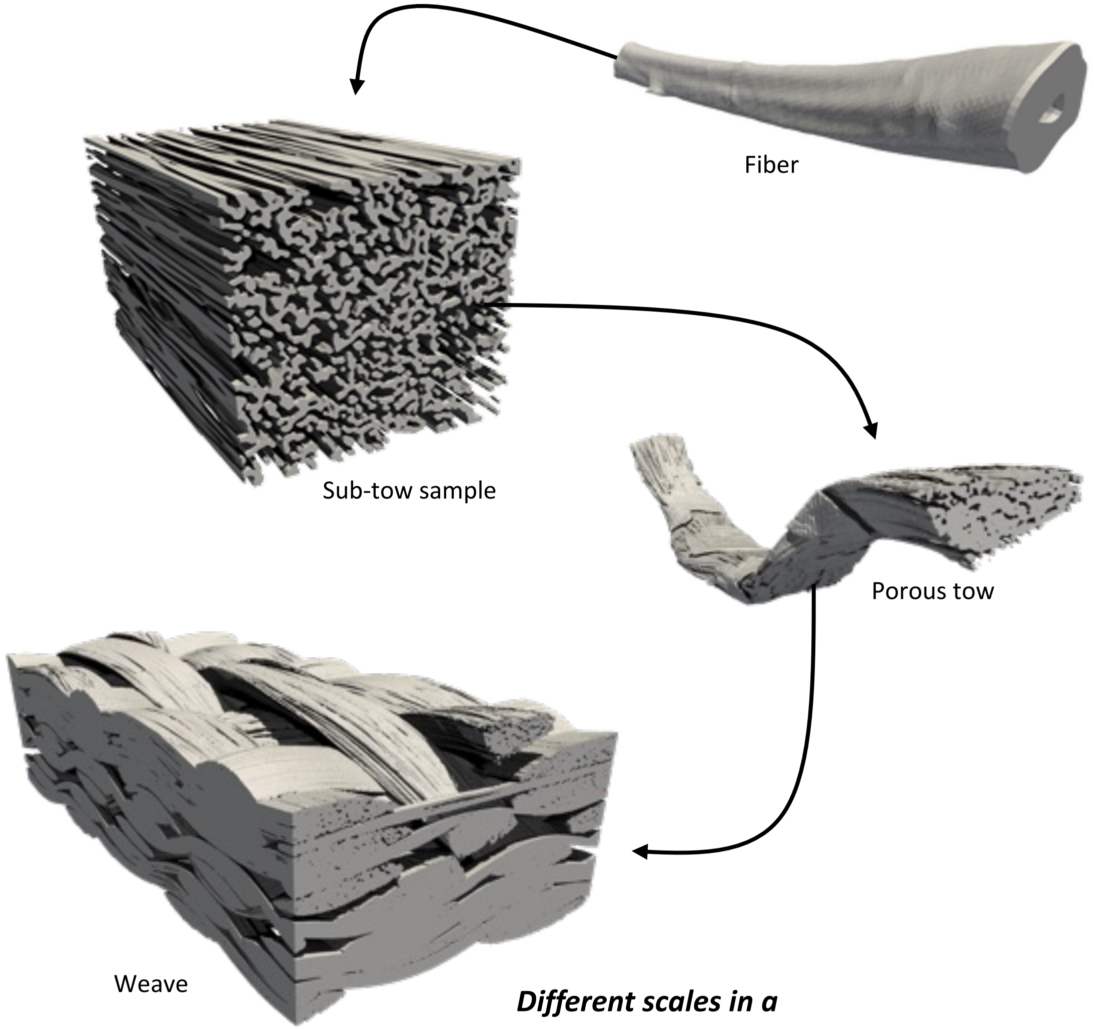

Different scales in a woven material

Woven TPS Multi-scale Modeling

- In 3D woven composites, some yarns are also weaved through the thickness direction.
- Designing this type of composite for specific applications is not trivial due to the high number of design options.
- This study focuses on multi-scale modeling to obtain the mechanical properties of different 3D woven composites.
  - Modeling steps: Matrix $\rightarrow$ Yarn $\rightarrow$ Unit Cell
- Use of PuMA's voxel-based thermal conductivity and stress analysis solver for anisotropic materials.
  - Finite volume
  - Cell-centered discretization

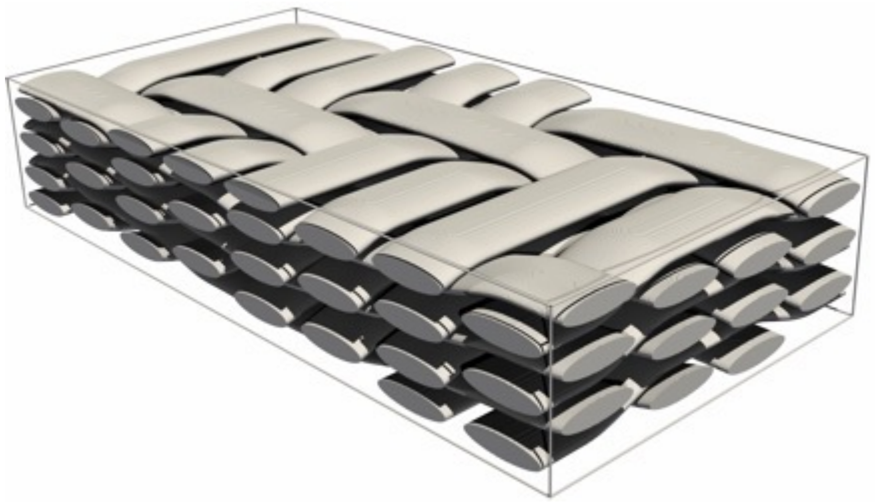

3D weave structure

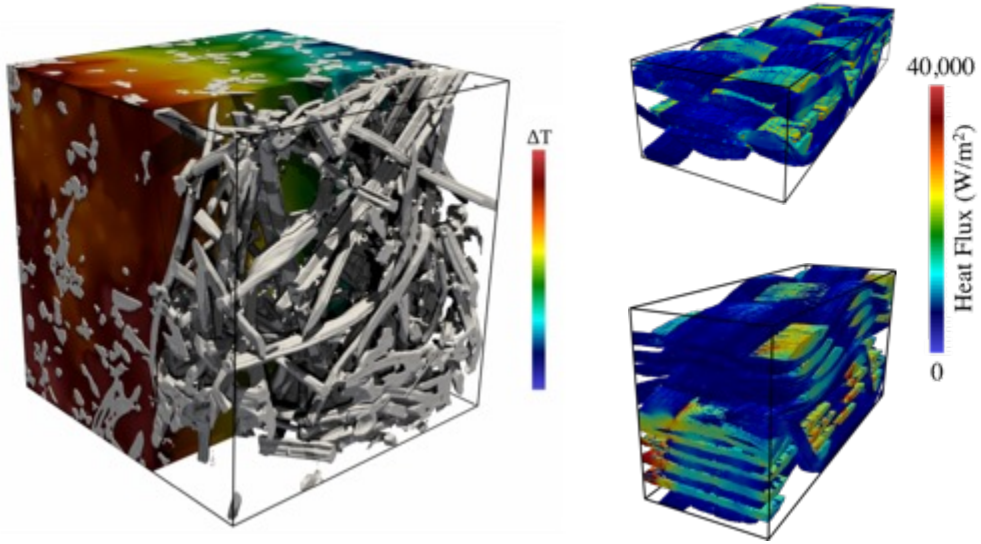

Heat transfer in fibrous material

Tools Overview: PuMA

- The PuMA software is able to either generate domains artificially or import them from micro-CT scans and compute material properties such as: porosity, specific surface area, effective thermal conductivity, pore diameter, tortuosity, permeability. It also enables the computation of mechanical properties though its anisotropic elasticity solver.

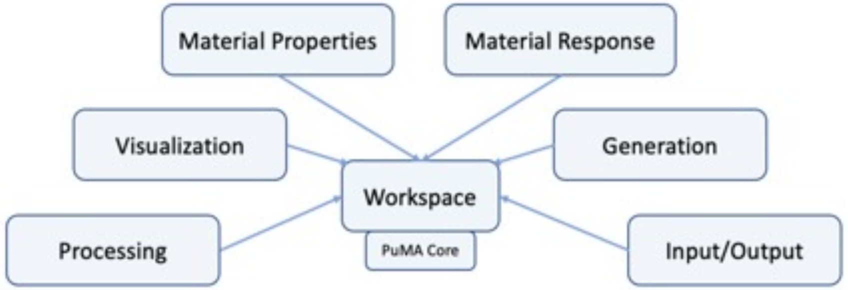

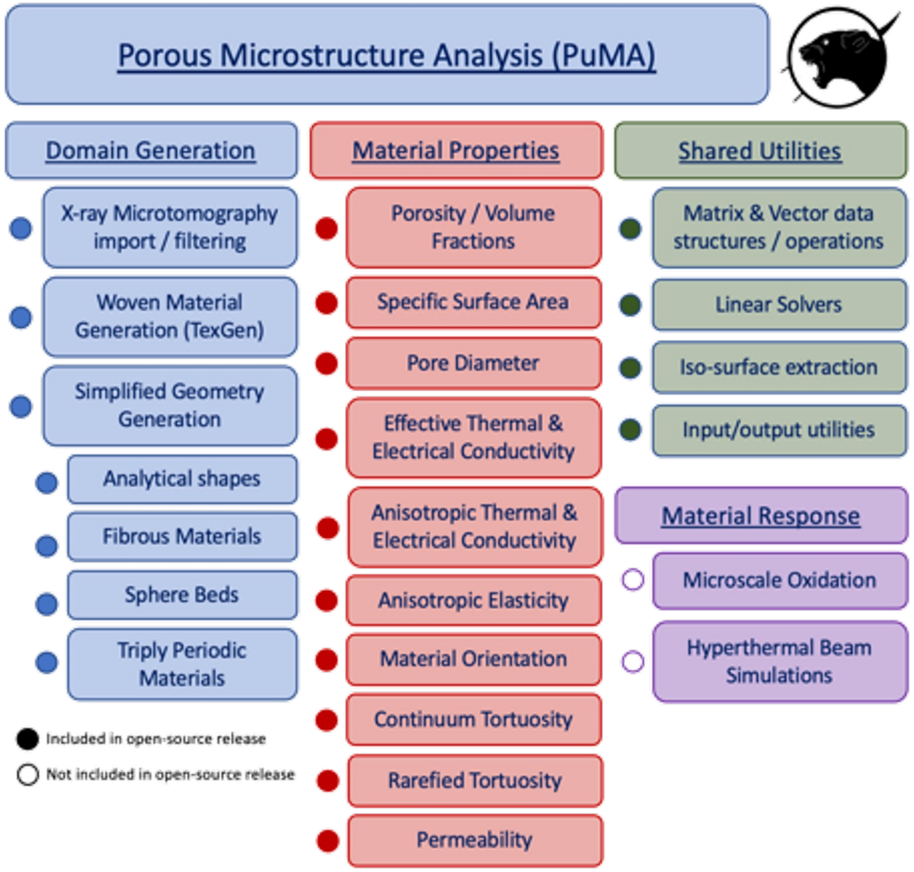

Tools Overview: PuM

- **Lead developers:** J.C. Ferguson and F. Semeraro
- **Installation:** conda install -c conda-forge puma
- **Open-source repository:** https://github.com/nasa/puma
- **Documentation:** https://puma-nasa.readthedocs.io
- **Community chat:** https://gitter.im/puma-nasa/community
- **Tutorials:** YouTube channel and Colab notebook

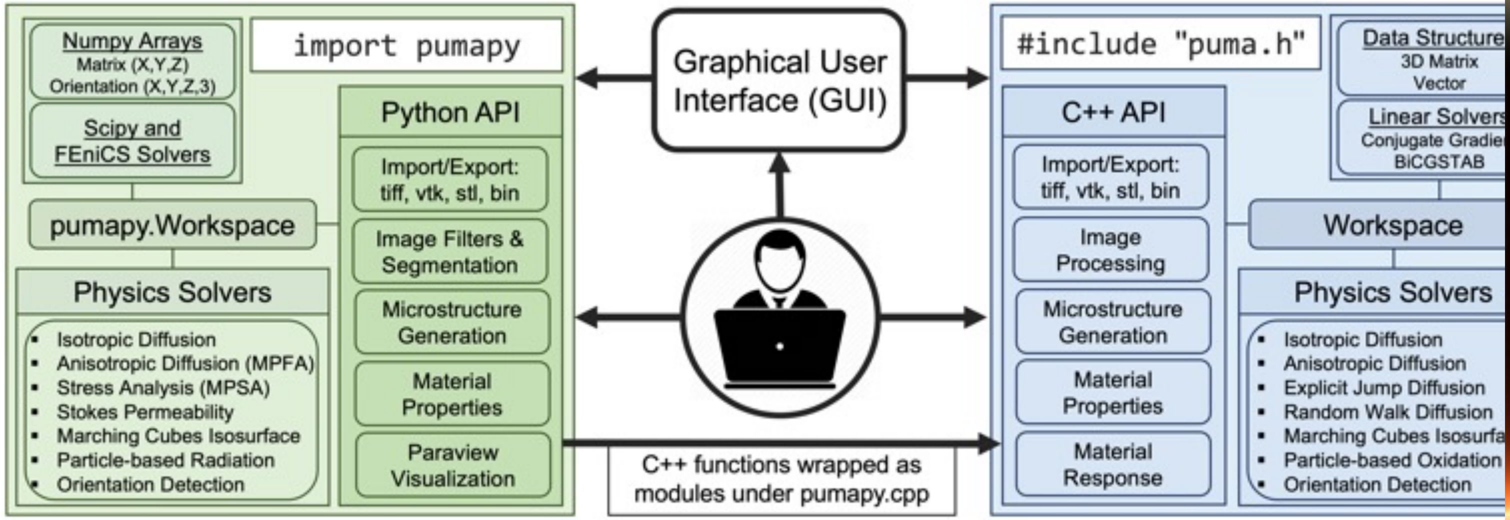

PuMA architecture diagram

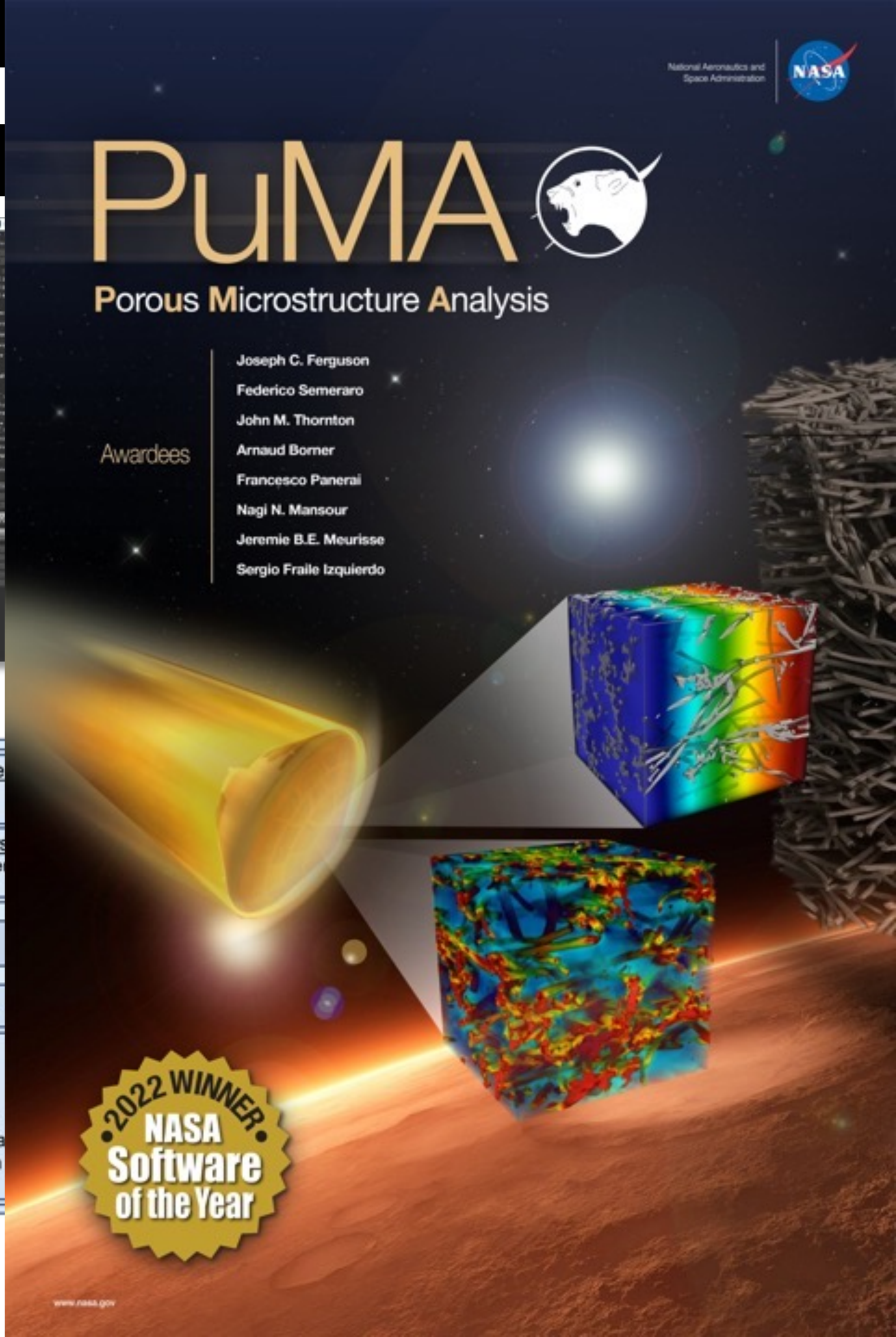

Tools Overview: TomoSAM

- An extension of 3D Slicer using the Segment Anything Model (SAM) from Meta to aid the segmentation of 3D data from tomography or other imaging techniques.
- **Lead developers:** F. Semeraro
- **Open-source repository:** https://github.com/fsemerar/SlicerTomoSAM

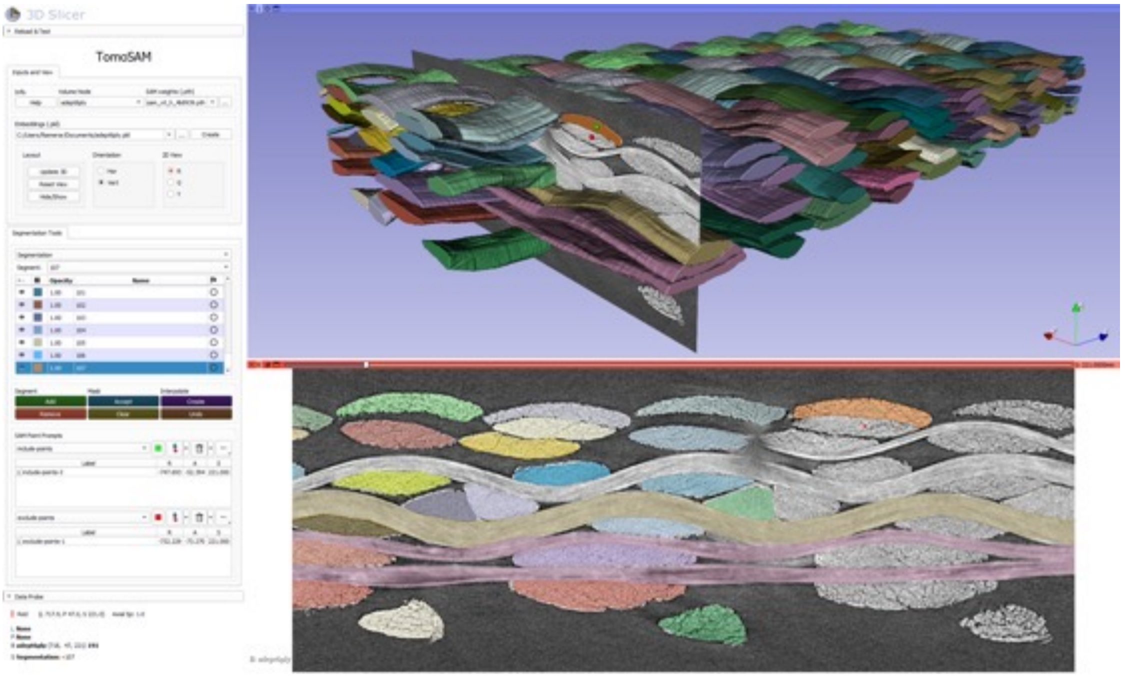

TomoSAM graphical user interface

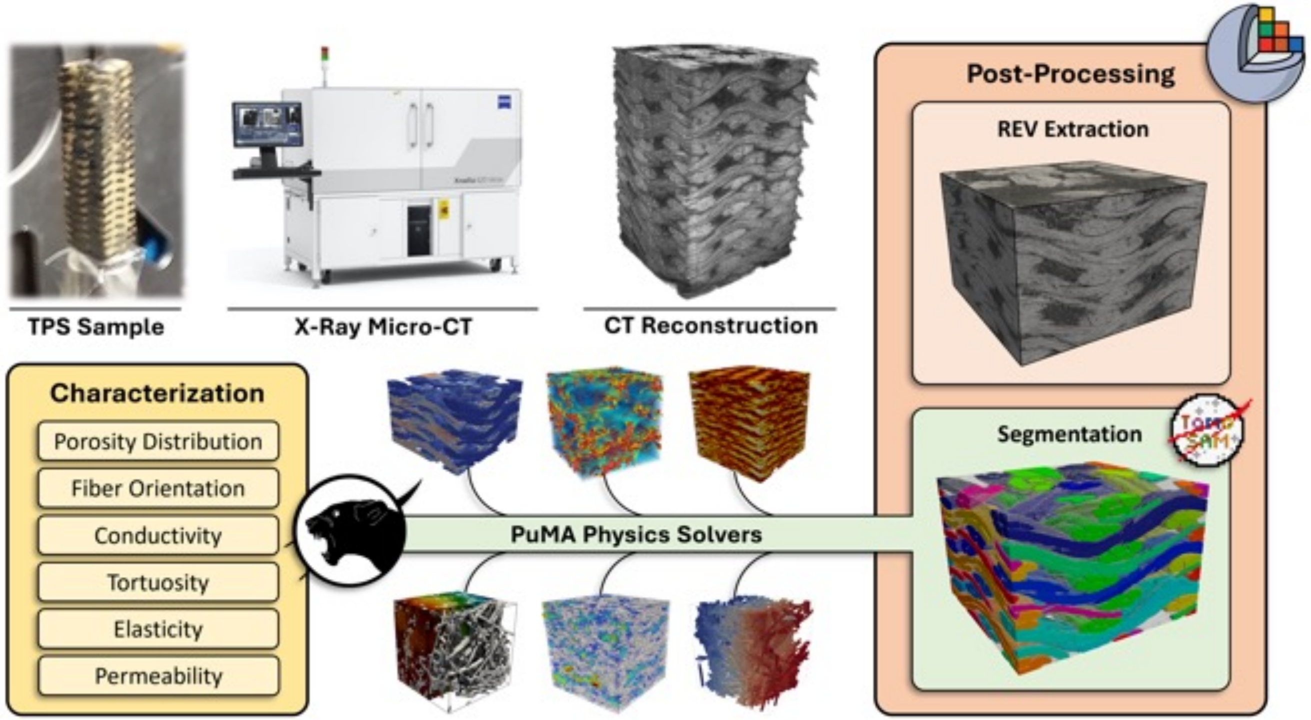

Micro-CT workflow diagram

Porous Matrix Modeling: Elasticity

Fully dense isotropic phenolic resin: E = 4.5 GPa, ν = 0.30

Random intersecting spherical pores: Φ = 0.0 / 0.2 / 0.4 / 0.6

Pore diameter sensitivity study: 4 – 20 voxels

Domain: 100 x 100 x 100 voxels

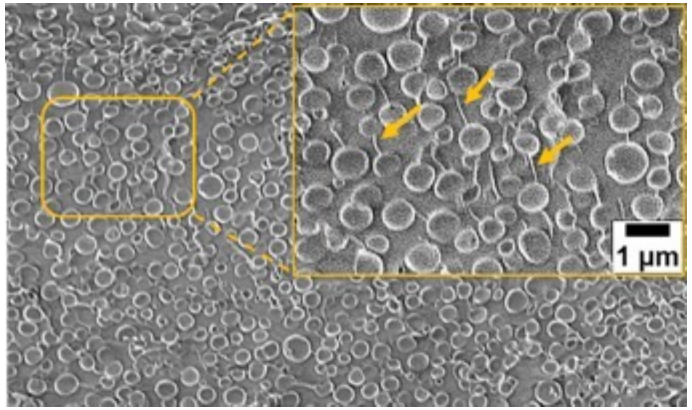

Fig.6 - Micrograph of cured porous phenolic resin [3]

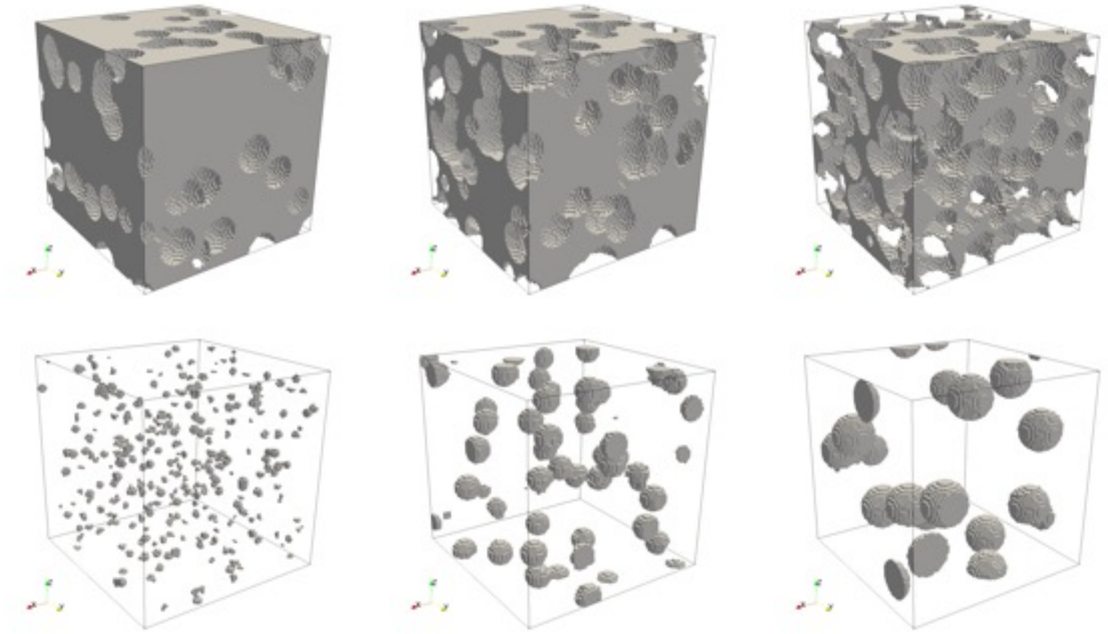

Fig.5 - Voxelized models of porous resin matrix (top) and different pore sizes (bottom)

Results compared with semi-empirical equations found in the literature:

- Bert: solid with spherical pores following a hexagonal distribution, ϕ_{max} = 0.7405 and c = 2 ϕ_{max} [4]
- Roberts: solid with random overlapping spherical pores, ϕ_{max} = 0.818 and c = 1.65 [5]

$$E_\phi = E_0 \left(1 - \frac{\phi}{\phi_{max}}\right)^c$$

Porous Matrix Modeling: Elasticity

- Pore diameter of the simulations shown: D = 16 voxels
- Assumed isotropic material
- RVE homogenization method:
  - Model's face in XY plane fixed
  - Displacement of 1 voxel in +X
  - Symmetry BC in the other 4 faces
- Top: Displacement field (X)
- Bottom: Direct stress field (X)

$\Phi = 0.2$ $\Phi = 0.4$ $\Phi = 0.6$

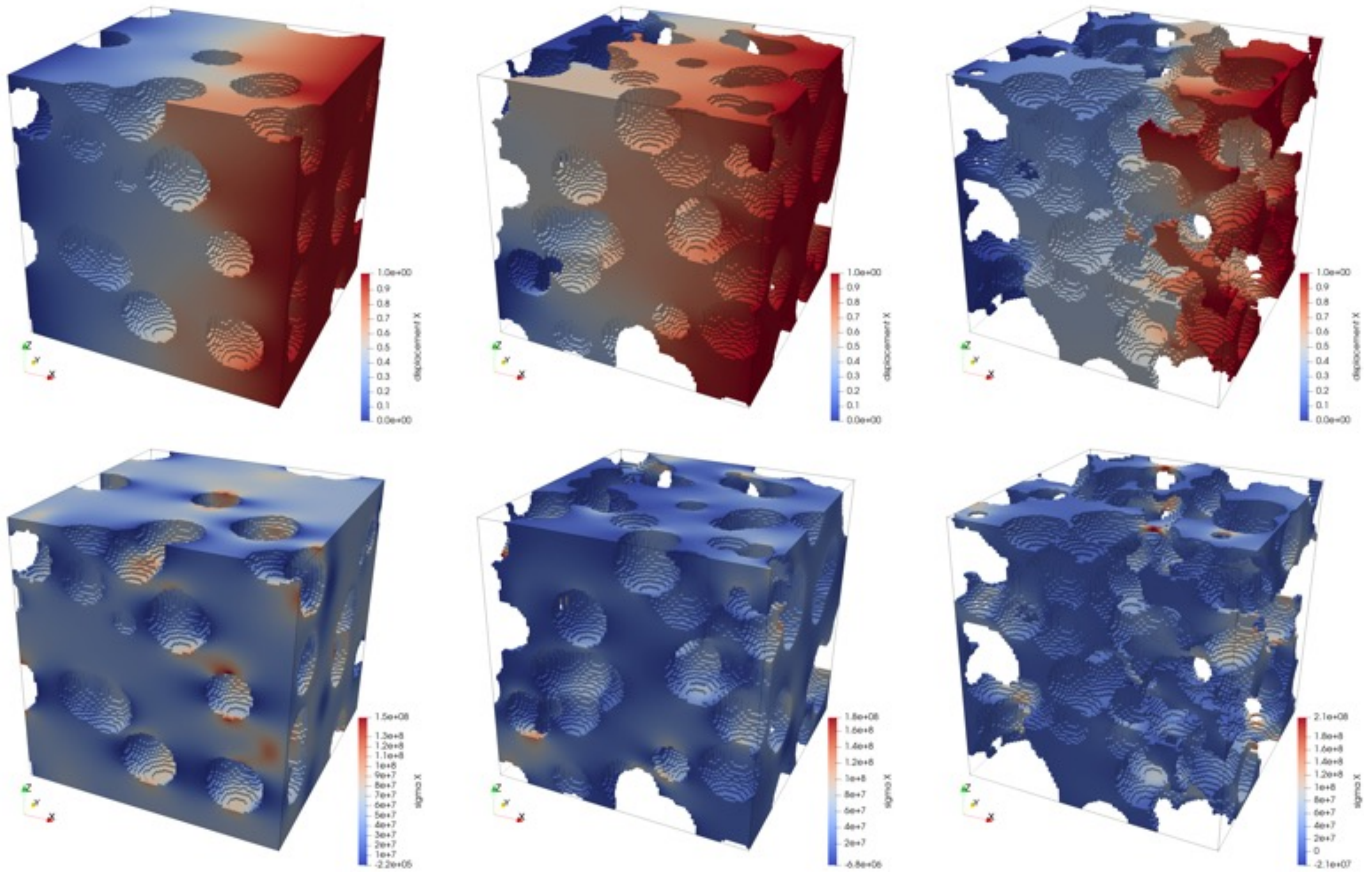

Displacement field (top) and direct stress field (bottom) in the X direction

Porous Matrix Modeling: Elasticity

- 9 pore diameters analyzed, up to 30 simulations each to minimize the random generation uncertainty.
- Pore diameter selected for this study: d = 20 voxels.
- Great agreement with Robert's equation.

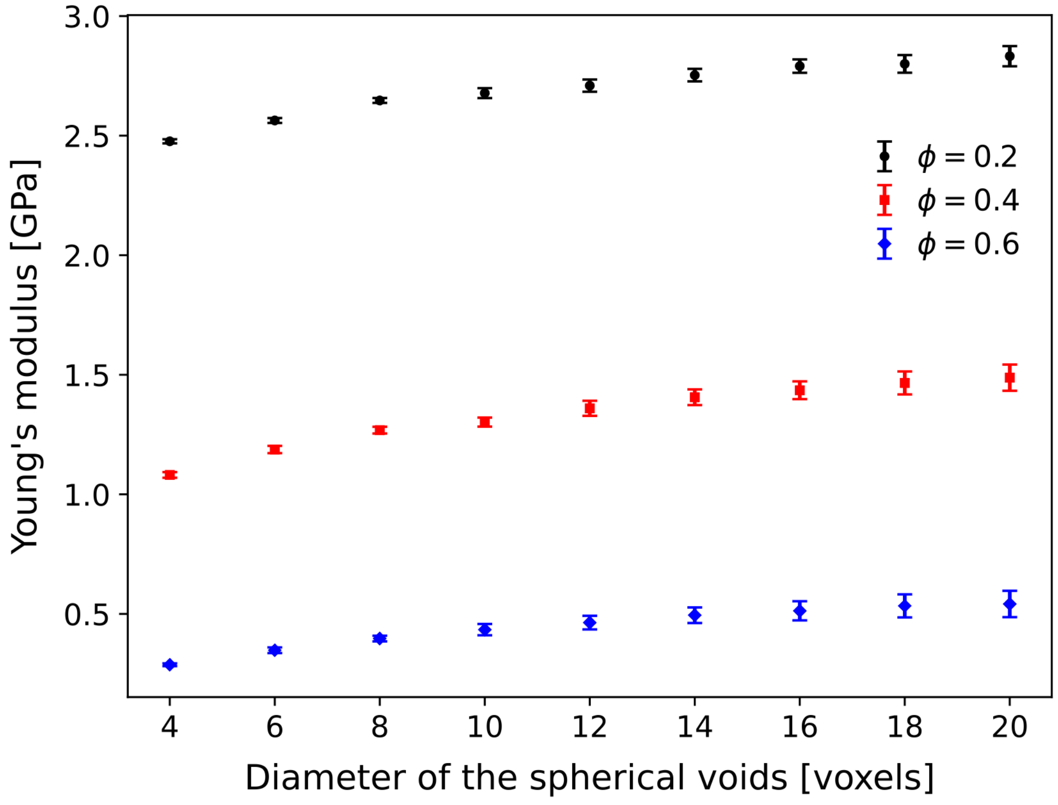

Young's moduli for different pore diameters and porosities

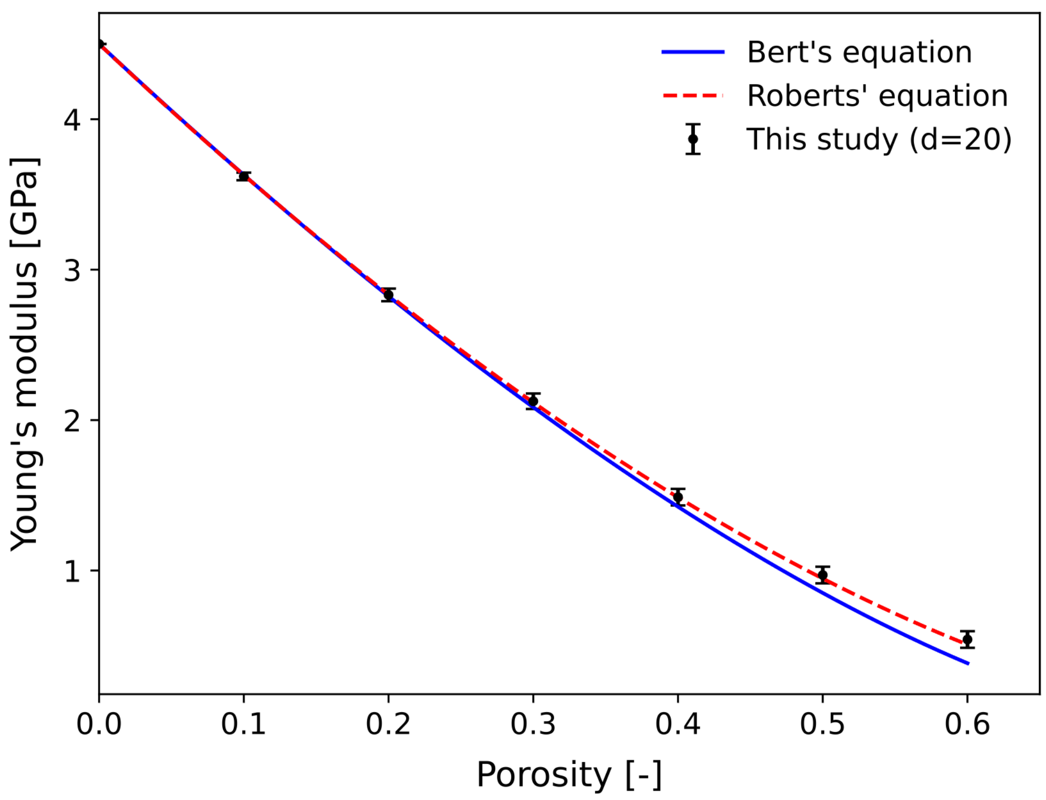

Young's moduli comparison for different porosities

Porous Matrix Modeling: Thermal Conductivity

- Porous phenolic model generated via random intersecting spherical voids.
- Fully dense isotropic phenolic resin (SC-1008): k = 0.25 W/mK
- Pores filled with air: k = 0.0257 W/mK
- Pore diameter = 20 voxels
- Domain = 300 x 300 x 300 voxels
- Multiple simulations Φ = [0 – 1]

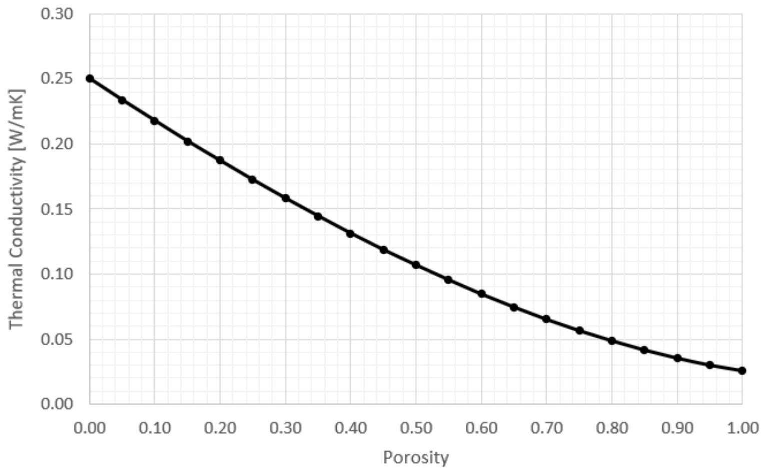

Phenolic resin thermal conductivity as function of porosity (PuMA)

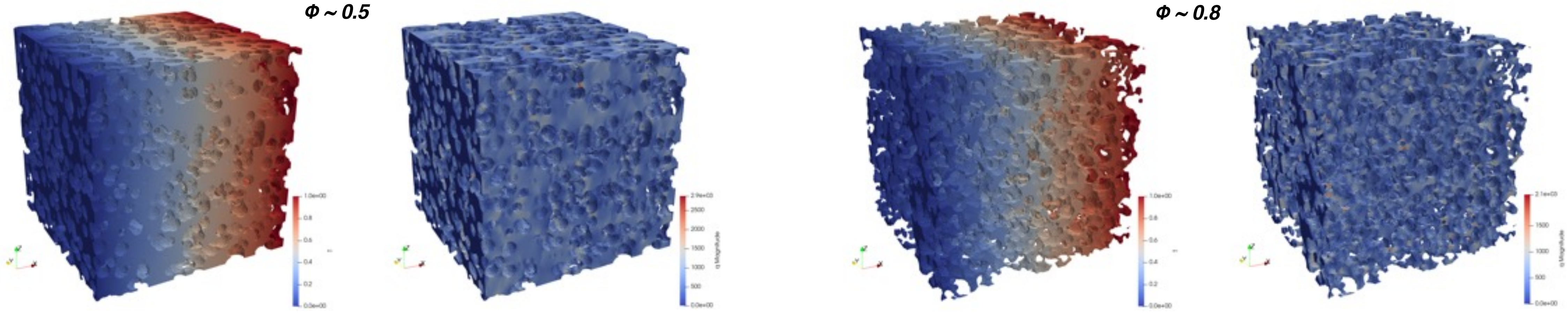

Temperature and heat flux fields for different porosity values

Tow Modeling: Artificially Generated – Elasticity

Yarns made of carbon and porous phenolic resin (hex distribution).

Porous phenolic: mechanical properties from this study, Φ = 0.0 - 0.6

Carbon fibers: E_L = 230 GPa, E_T = 15 GPa, ν_{LT} = 0.20, ν_{TT} = 0.20

Fiber volume fraction in tow: V_f = 0.5 / 0.6 / 0.7 / 0.8

Domain: 25 x 100 x 173 voxels

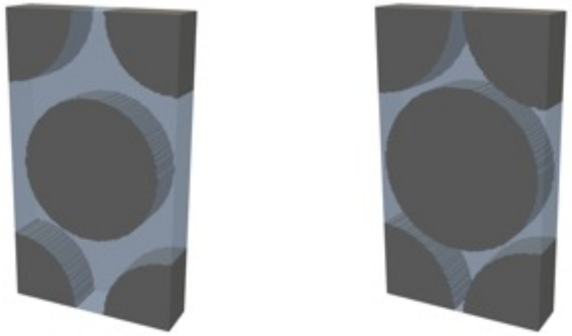

Voxelized tow models, V_f = 0.6, 0.8

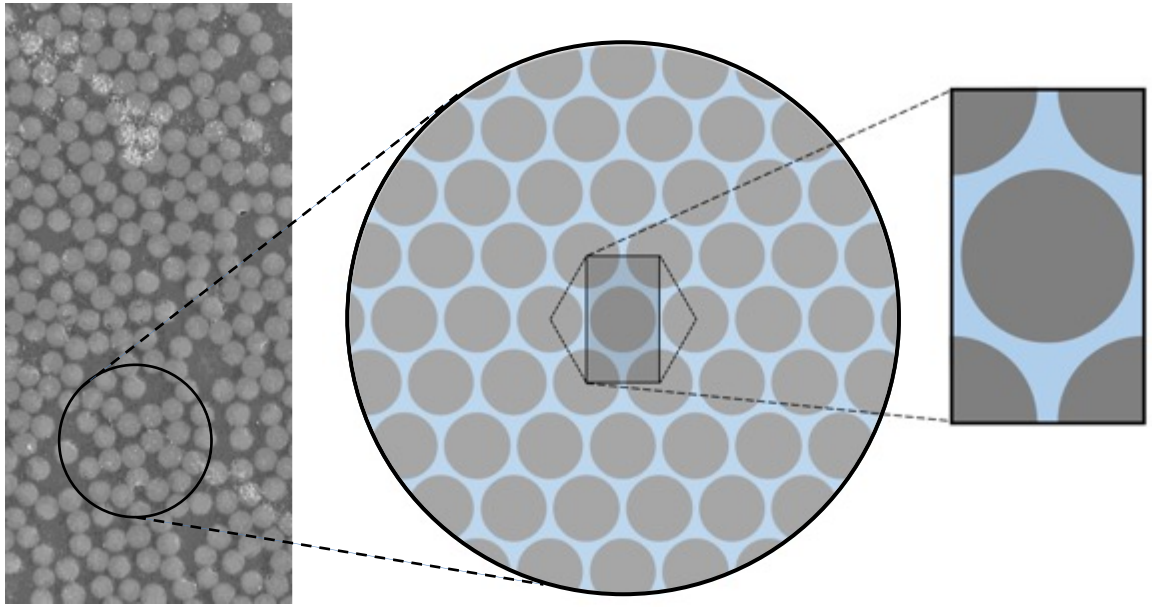

Micrograph of carbon fibers [6]

Results compared with theoretical and semi-empirical equations found in the literature:

- Rule of Mixtures (ROM): good approximation for E_L and ν_{LT}
- Halpin-Tsai: better approximation of E_T than ROM with empirical parameter for hex distribution ξ = 1 (η = 1) [7]
- Nielsen: modified Halpin-Tsai equation with maximum fiber packing parameter η = 0.907 [8]
- Chamis: widely used due its simplicity and greater accuracy compared to ROM [9]

Tow Modeling: Artificially Generated – Elasticity

Yarns made of carbon and porous phenolic resin (hex distribution).

Porous phenolic: mechanical properties from this study, $\Phi = 0.0 - 0.6$

Carbon fibers: $E_L = 230$ GPa, $E_T = 15$ GPa, $\nu_{LT} = 0.20$, $\nu_{TT} = 0.20$

Fiber volume fraction in tow: $V_f = 0.5 / 0.6 / 0.7 / 0.8$

Domain: 25 x 100 x 173 voxels

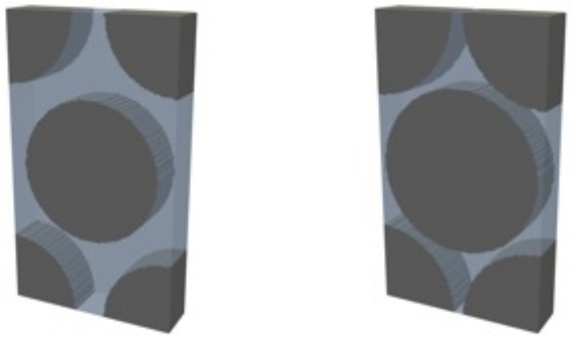

Voxelized tow models, V_f = 0.6, 0.8

ROM

$$E_L = E_{f_L} V_f + E_m V_m \qquad \nu_{LT} = \nu_{f_{LT}} V_f + \nu_m V_m$$

Halpin-Tsai
Nielsen

$$E_T = E_m \frac{1 + \xi \eta V_f}{1 - \psi \eta V_f} \quad \textit{where,} \quad \eta = \frac{r - 1}{r + \xi} \qquad r = \frac{E_{f_T}}{E_m}$$

Chamis

$$E_T = \frac{E_m}{1 - \sqrt{V_f}\left(1 - \frac{E_m}{E_{f_T}}\right)}$$

Results compared with theoretical and semi-empirical equations found in the literature:

- Rule of Mixtures (ROM): good approximation for E_L and ν_{LT}
- Halpin-Tsai: better approximation of E_T than ROM with empirical parameter for hex distribution $\xi = 1$ ($\eta = 1$) [7]
- Nielsen: modified Halpin-Tsai equation with maximum fiber packing parameter $\eta = 0.907$ [8]
- Chamis: widely used due its simplicity and greater accuracy compared to ROM [9]

Tow Modeling: Artificially Generated – Elasticity

- Fully dense phenolic matrix for the simulations shown.
- RVE homogenization method:
  - Model's face in XY plane fixed
  - Displacement of 1 voxel in +Z
  - Periodic BC in the other 4 faces
- Top: Displacement field (Z)
- Bottom: Direct stress field (Z)

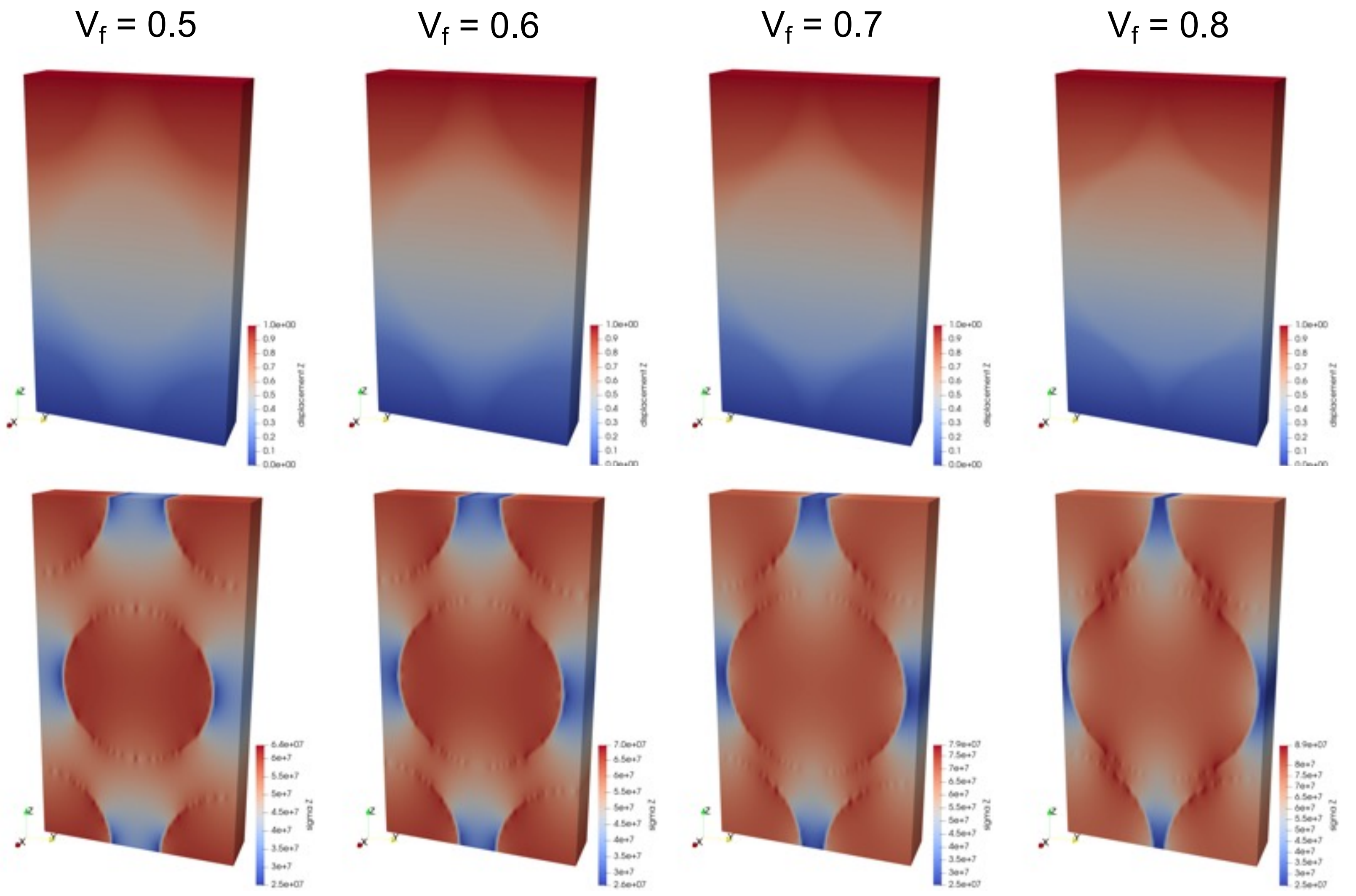

Displacement field (top) and direct stress field (bottom) in the Z direction

Tow Modeling: Artificially Generated – Elasticity

- Halptin-Tsai shows the best agreement with the results from PuMA for E_T

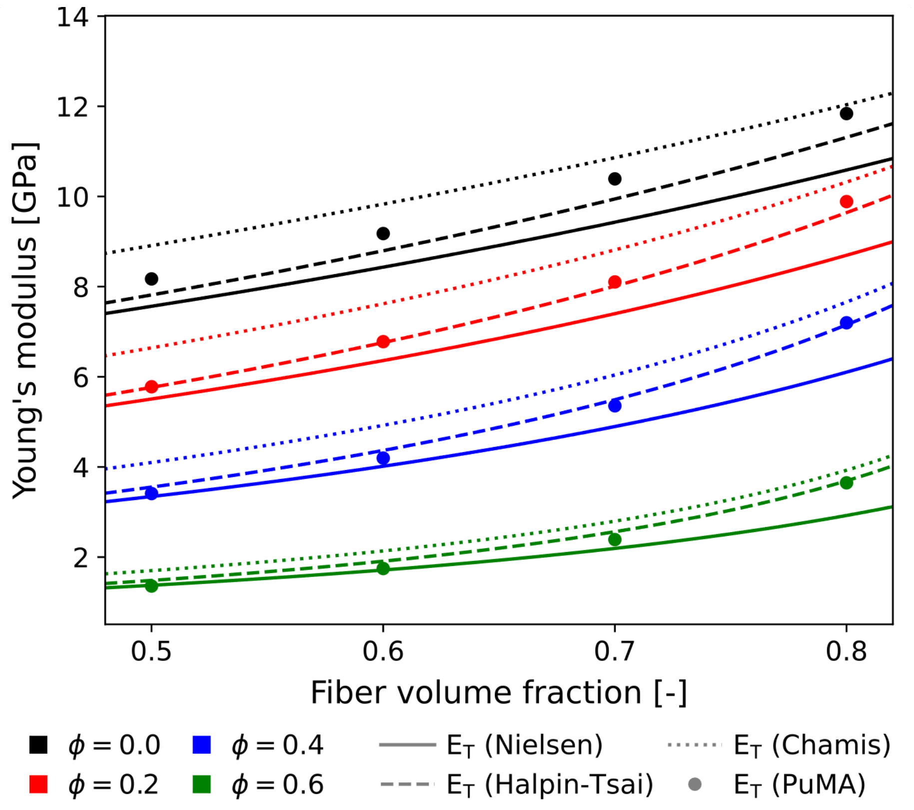

Fig.16 - Yarns Transverse Young's modulus

- ROM shows great agreement with results from PuMA for E_L and ν_{LT}

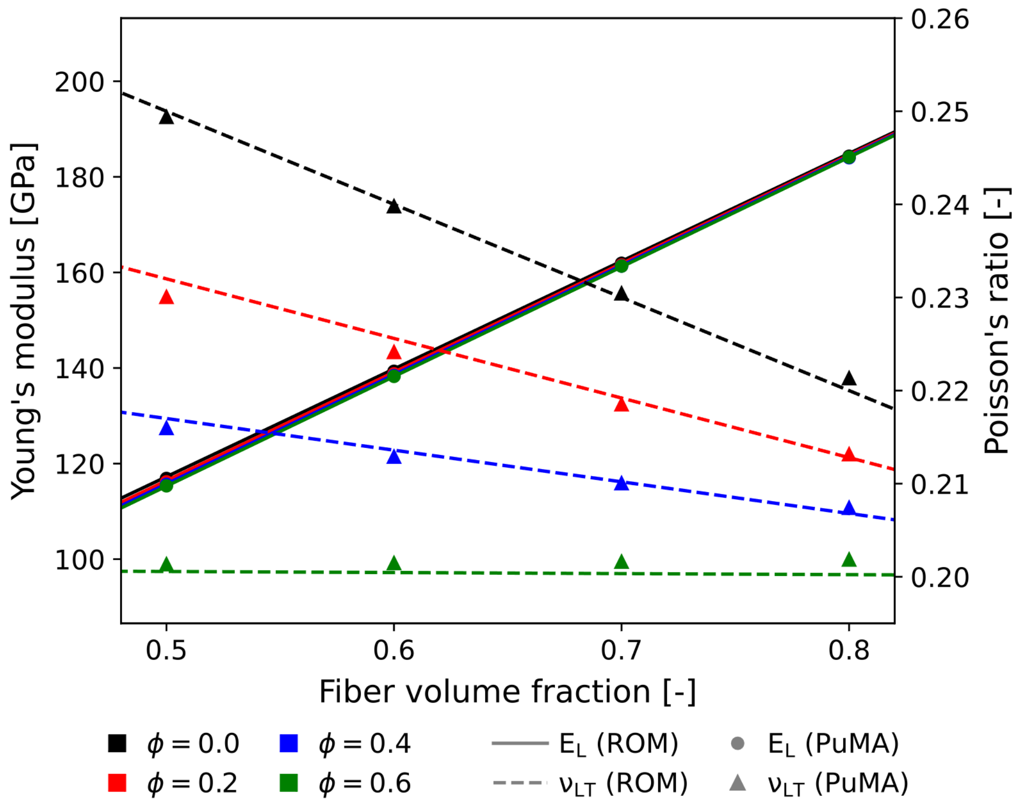

Fig.17 - Longitudinal Young's modulus and Poisson's ratio

Tow Modeling: Microscopy – Thermal Conductivity

- Segmentation of HEEET-IL microscopy images is important to obtain more accurate material properties and composition data of the TPS constituents.
- A UNet CNN was trained to automate the segmentation process leveraging Dragonfly's Deep Learning capabilities.
- Approach followed for the segmentation:
  - Mask out the in-plane tows to clean up the images and train the UNet CNN only with the through-thickness tows.
  - Segment manually a few regions to start training the UNet CNN and use the initial model's predictions to help with the segmentation of additional regions.
  - Correct the segmentation of the predicted labels and continue training the UNet model with the new data.
  - Continue the process with different microscopy images to generate additional training data.

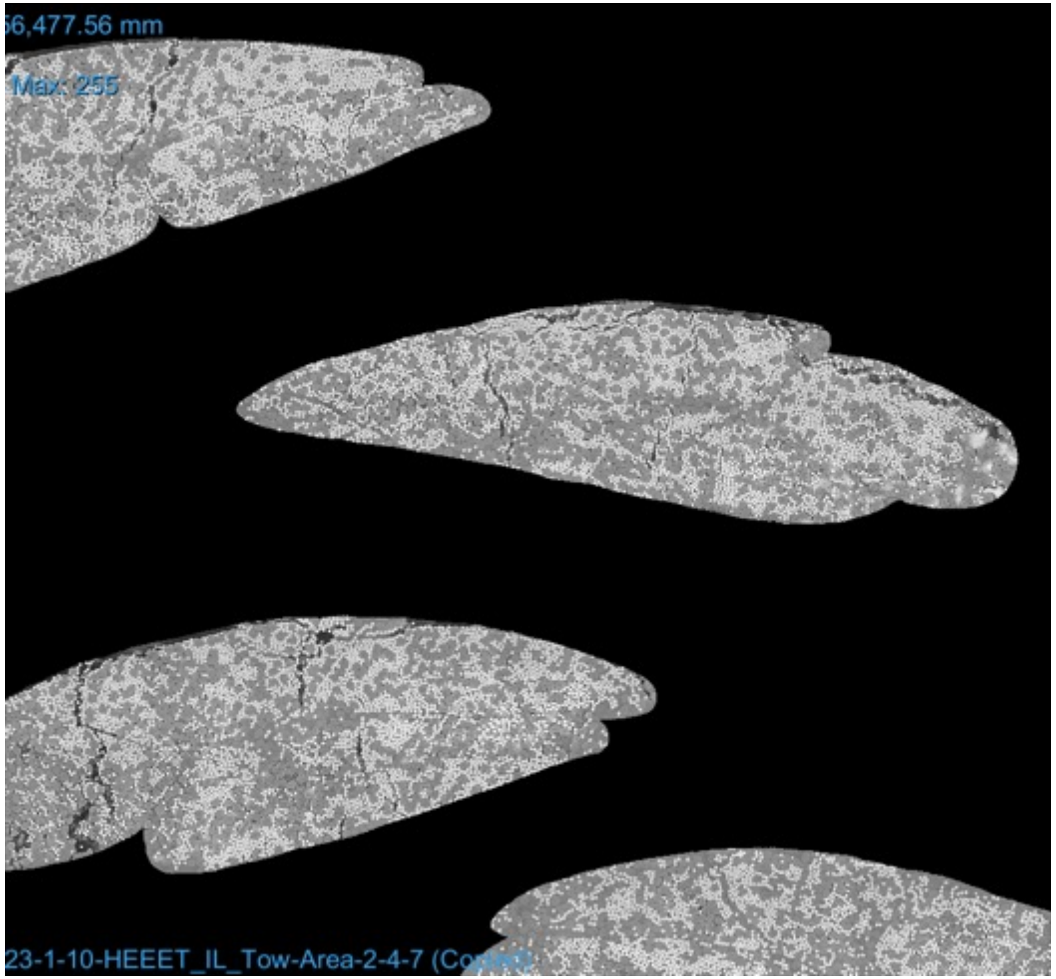

HEEET-IL microscopy image (NASA-GRC) though the steps of masking out the in-plane tows

Tow Modeling: Microscopy – Thermal Conductivity

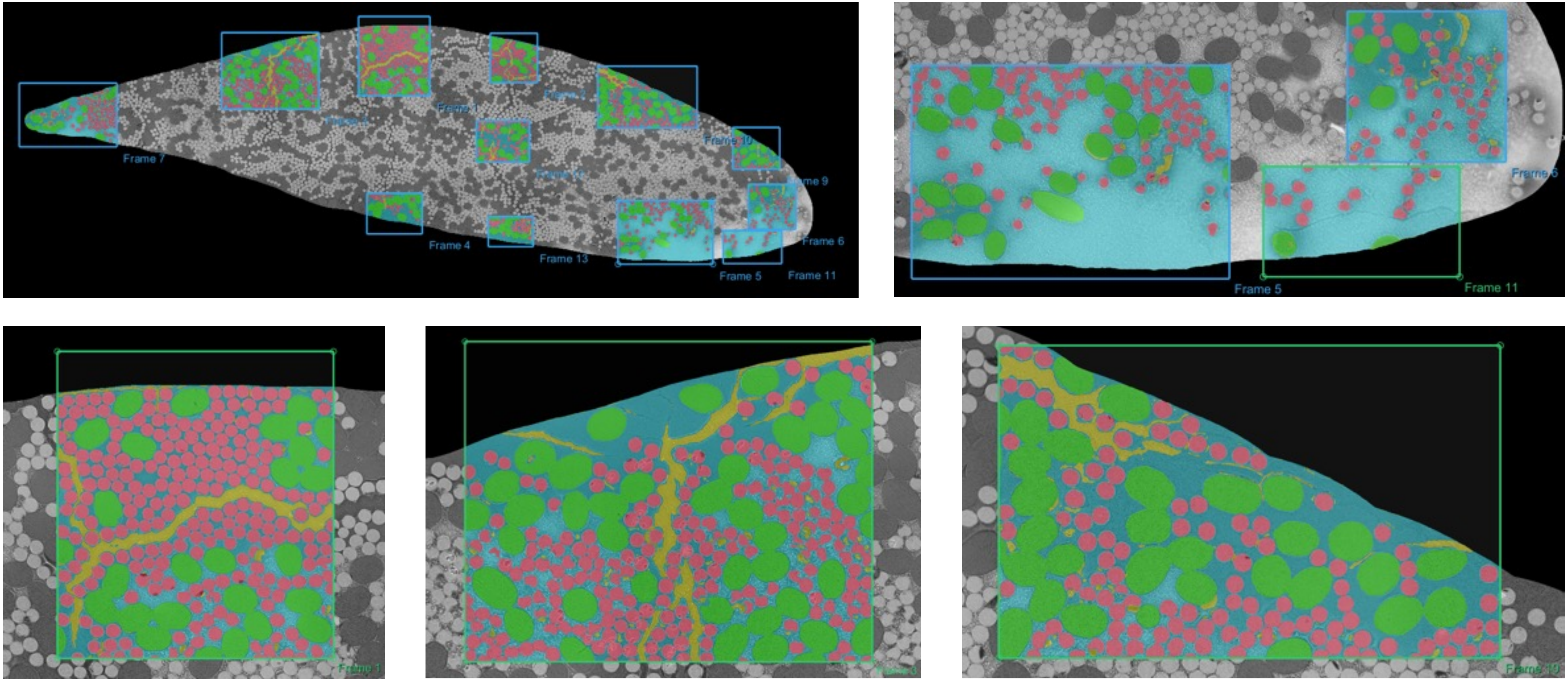

Selection of regions segmented of the HEEET-IL microscopy image (NASA-GRC) to train the UNet CNN

Tow Modeling: Microscopy – Thermal Conductivity

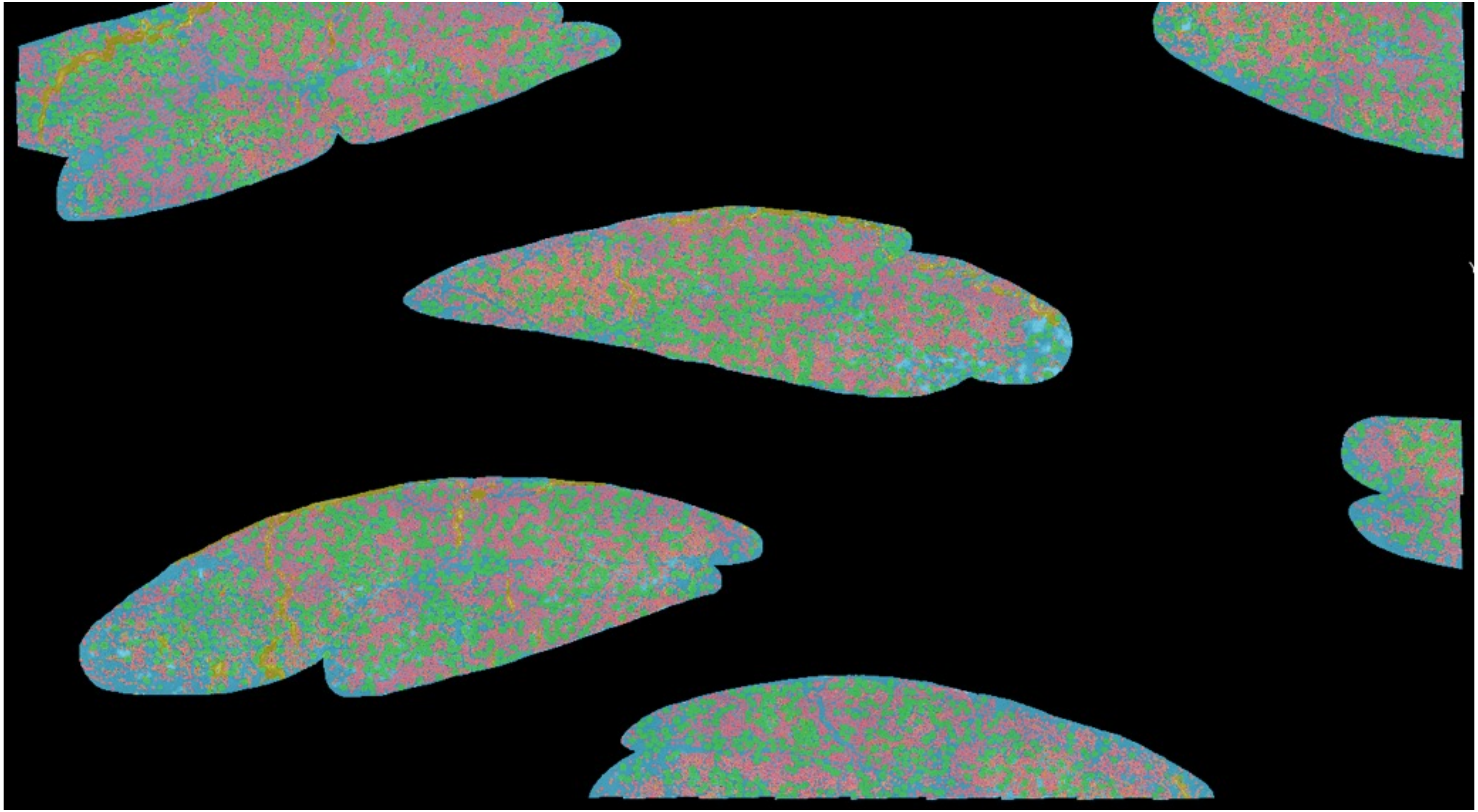

Segmented microscopy image using the trained UNet model

Tow Modeling: Microscopy – Thermal Conductivity

- Once the microscopy data is fully segmented, PuMA can calculate the average thermal conductivity of a tow.
- Selected 75 regions or "frames" of sizes between 500^2 and 1600^2 pixels for thermal conductivity evaluation.

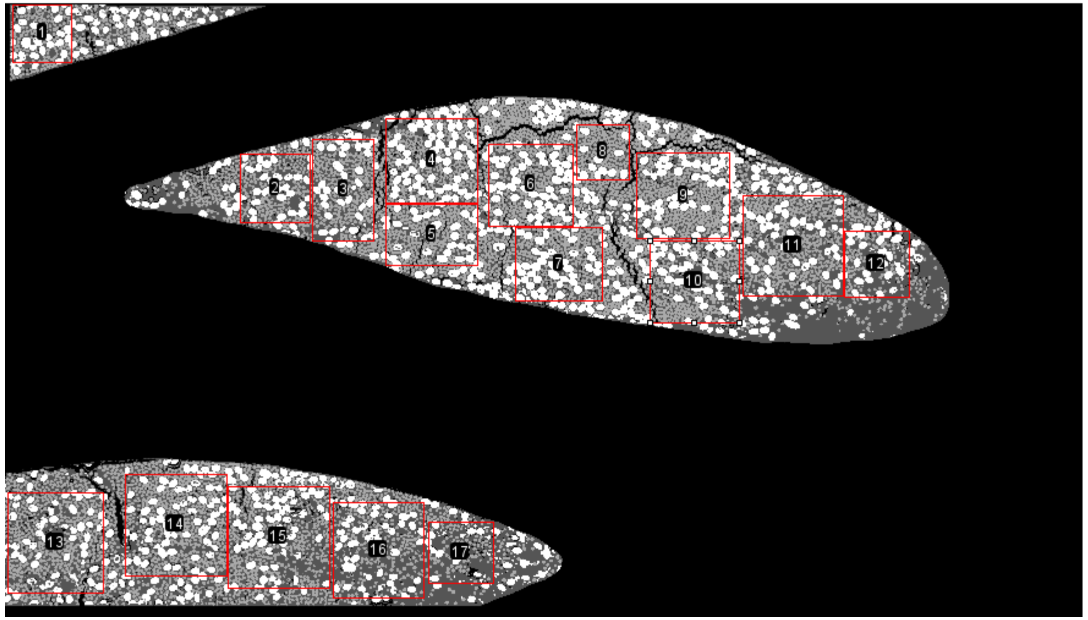

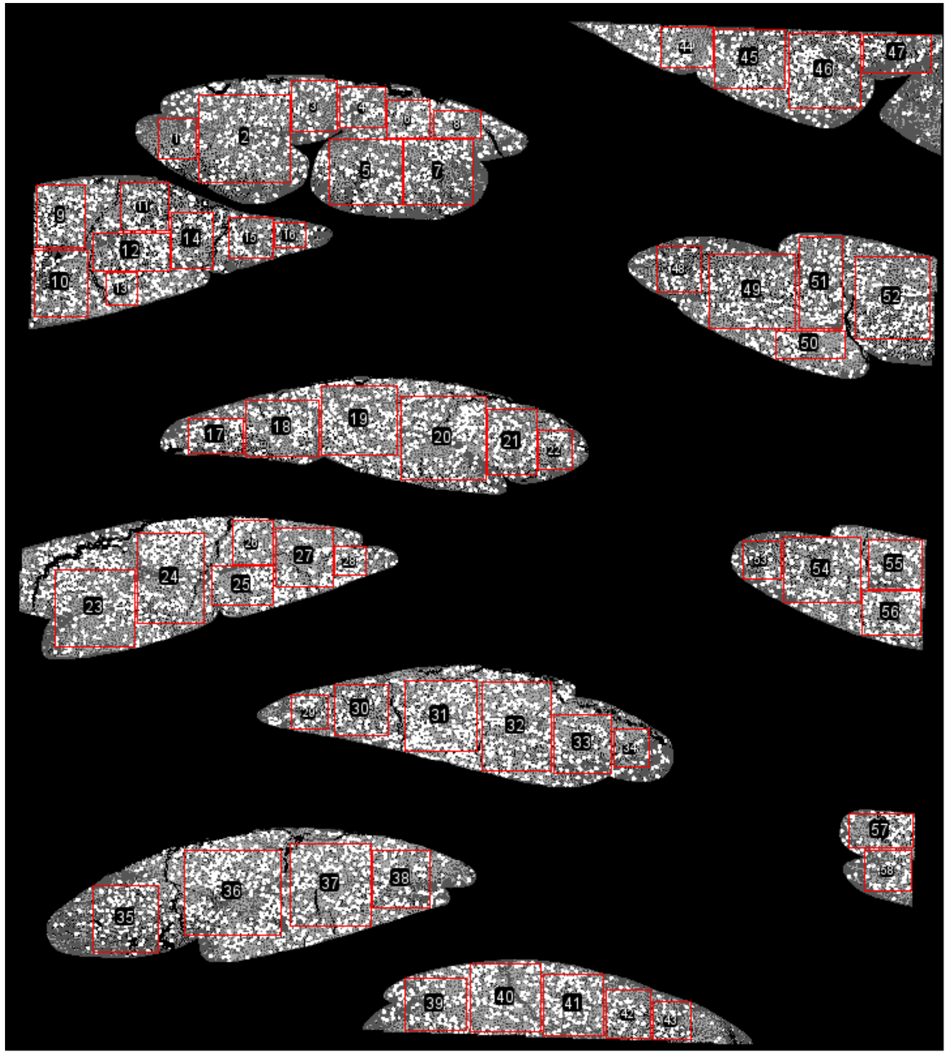

Frames selected for thermal conductivity calculation, 2023-1-10-HEEET_IL_Warp_L2 (left) and 2023-1-10-HEEET_IL_Tow-Area-2-4-7 (right)

Tow Modeling: Microscopy – Thermal Conductivity

- AS4 carbon fiber: k_{axial} = 6.9 W/mK, $k_{transverse}$ = 2.52 W/mK
- Phenolic fiber assumed fully dense phenolic resin: k = 0.25 W/mK
- Porosity of infiltrated phenolic resin considered.
- Final conductivity value computed by volume averaging the results for all frames.

Tow Properties	Value
VF Cracks	
VF Phenolic Resin	
VF Carbon Fibers	
VF Phenolic Fibers	
$k_{transverse}$	
k_{axial}	

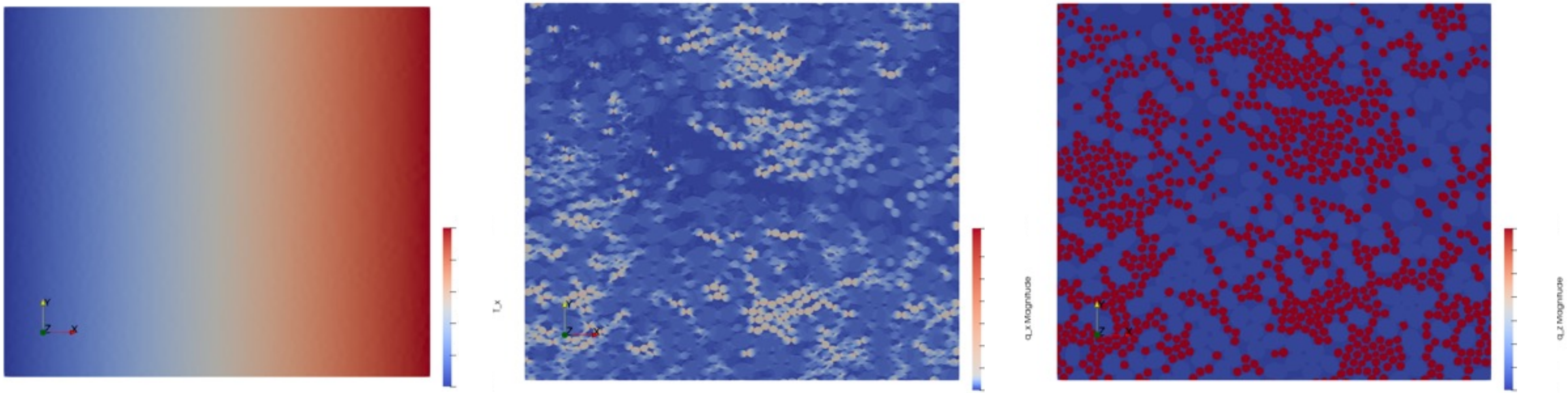

HEEET_IL_Tow-Area-2-4-7 frame #36, temperature_x (left), heat flux_x (center) and heat flux_z (right) fields.

Ji, X. *et al. Carbon* **2022**, *197*, 1–9.

Unit Cell: Micro-CT Data

- Micro-CT data provided by Kyle Hendrickson, infused sample “HEEET-24-016-001-12”
- Sample object of this study taken from the middle section of the reconstructed image.
- Tows made of four twisted sub-tows, and visible matrix cracks.
- Sample resolution:
  - X (R) - 472px (Fill)
  - Y (A) - 497px (Warp)
  - Z (S) - 330px (Thickness)

Raw and cropped micro-CT data

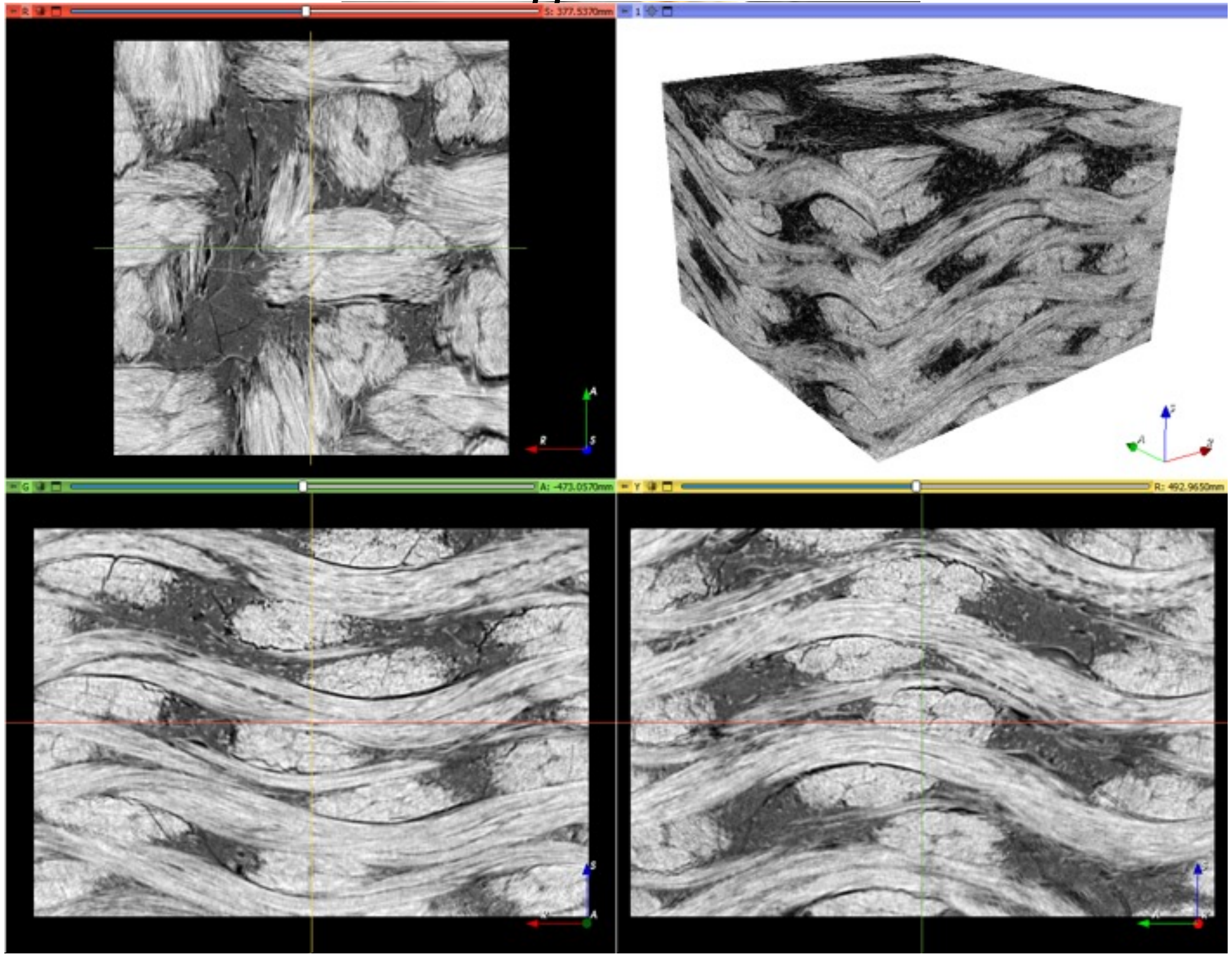

HEEET-24-016-001-12 sample (credits: Kyle Hendrickson)

Unit Cell: Micro-CT Segmentation

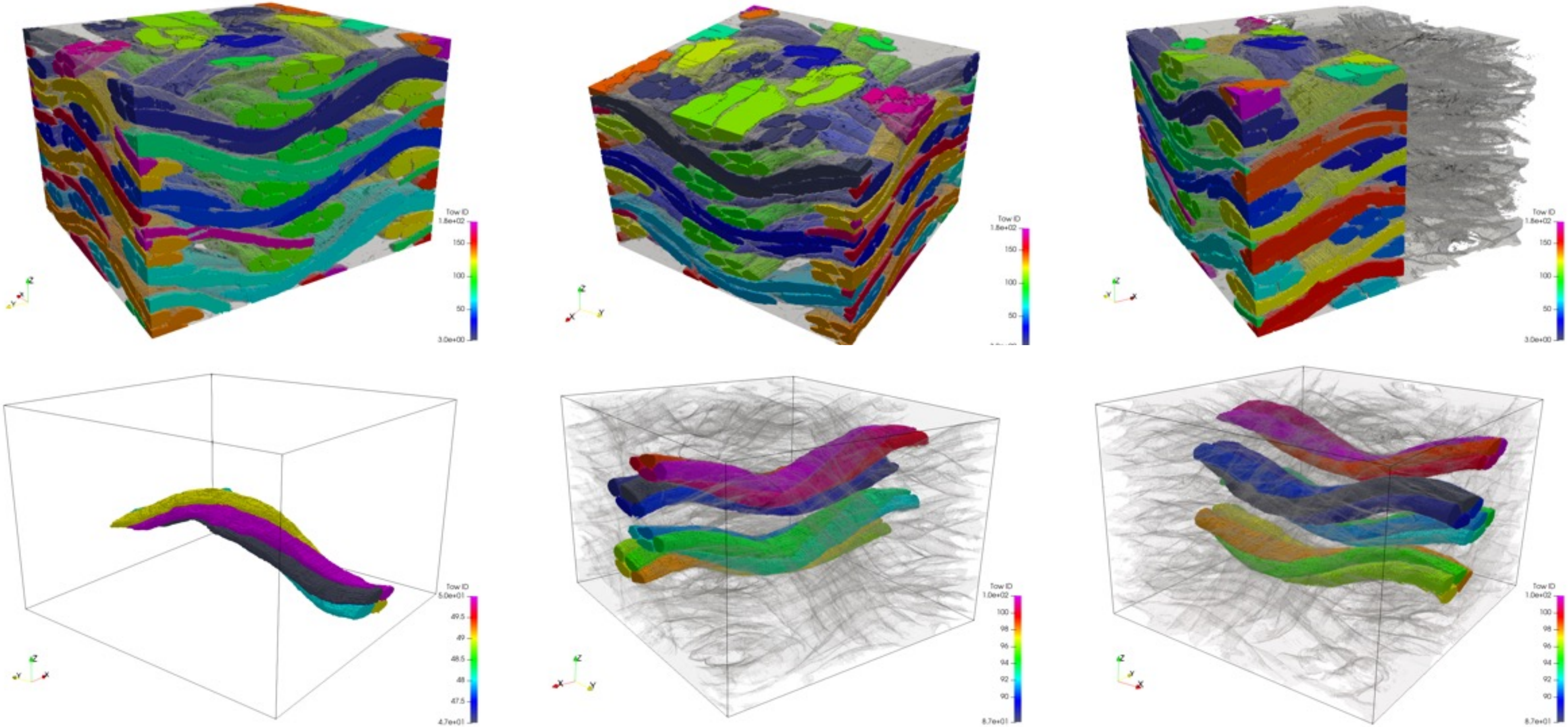

Segmented 3MDCP visualizations

Unit Cell: Micro-CT Orientation

- Orientation of the tows computed for the full resolution micro-CT data.
- Orientation fields are important to apply different mechanical properties or thermal conductivity values along and across the sub-tows.
- Tow's orientation computed using PuMA's Structure Tensor method for each tow individually.
- Final orientation values obtained by averaging the results for each cross-section of each tow to reduce errors.

Sub-tows number 48, 59, 110 and 125

Unit Cell: Artificially Generated – Elasticity

Yarns: phenolic resin impregnated carbon fibers, V_f = 0.5 / 0.6 / 0.7 / 0.8

Matrix: porous phenolic resin, Φ = 0.0 / 0.2 / 0.4 / 0.6

Domain: 150 x 150 x 60 voxels

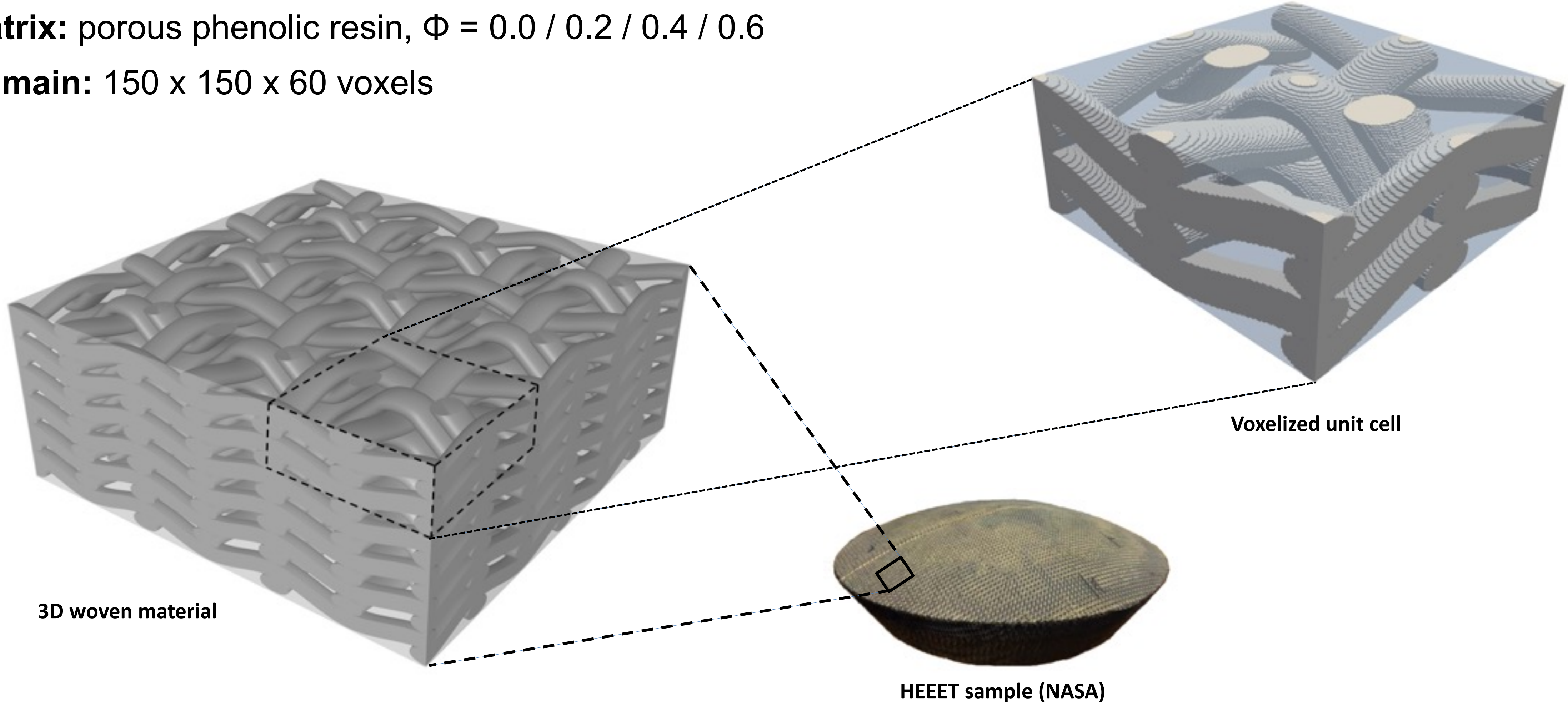

Unit Cell: Artificially Generated – Elasticity

- RVE homogenization method: displacement of 1 voxel in +X, +Y and +Z respectively with periodic BCs.

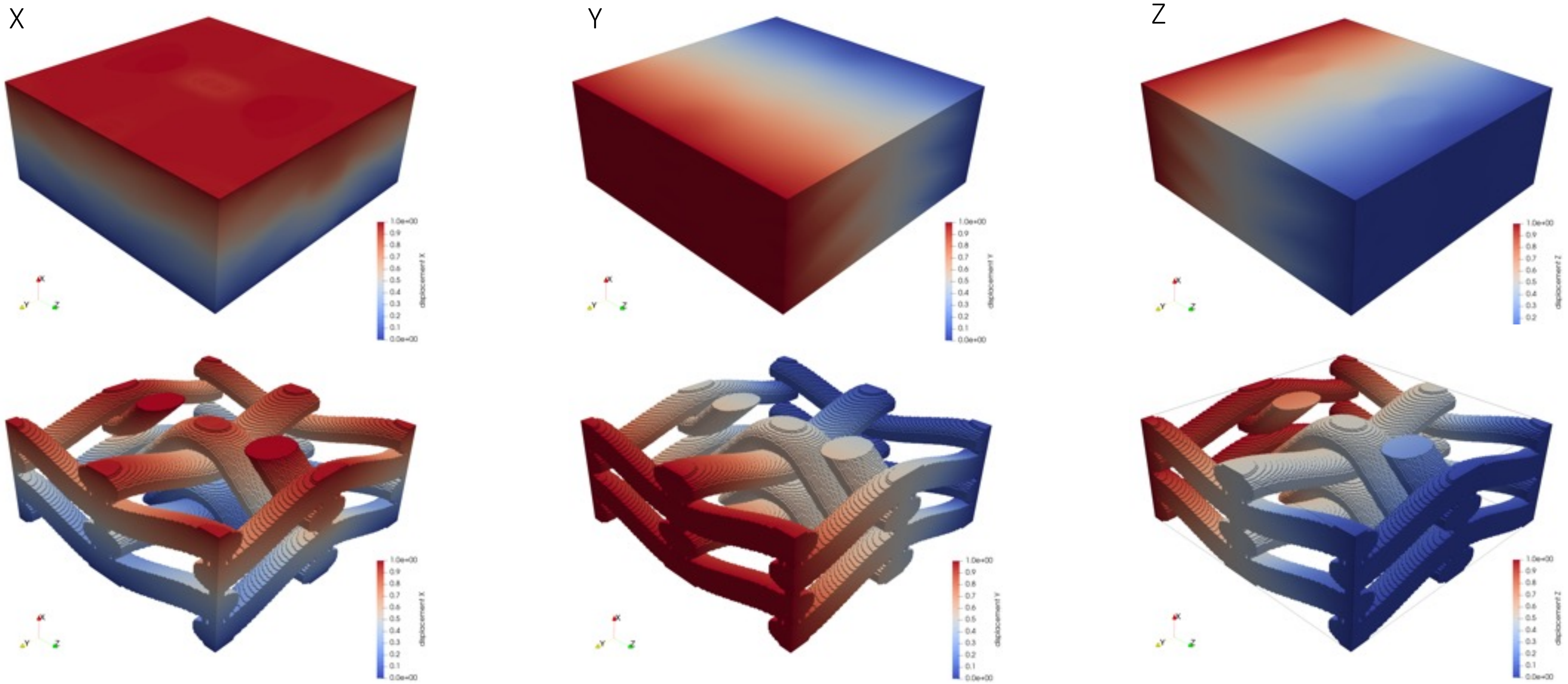

Fig.18 - Displacement field with matrix visible (top) and matrix hidden (bottom) in the X, Y and Z directions

Unit Cell: Artificially Generated – Elasticity

- RVE homogenization method: displacement of 1 voxel in +X, +Y and +Z respectively with periodic BCs.

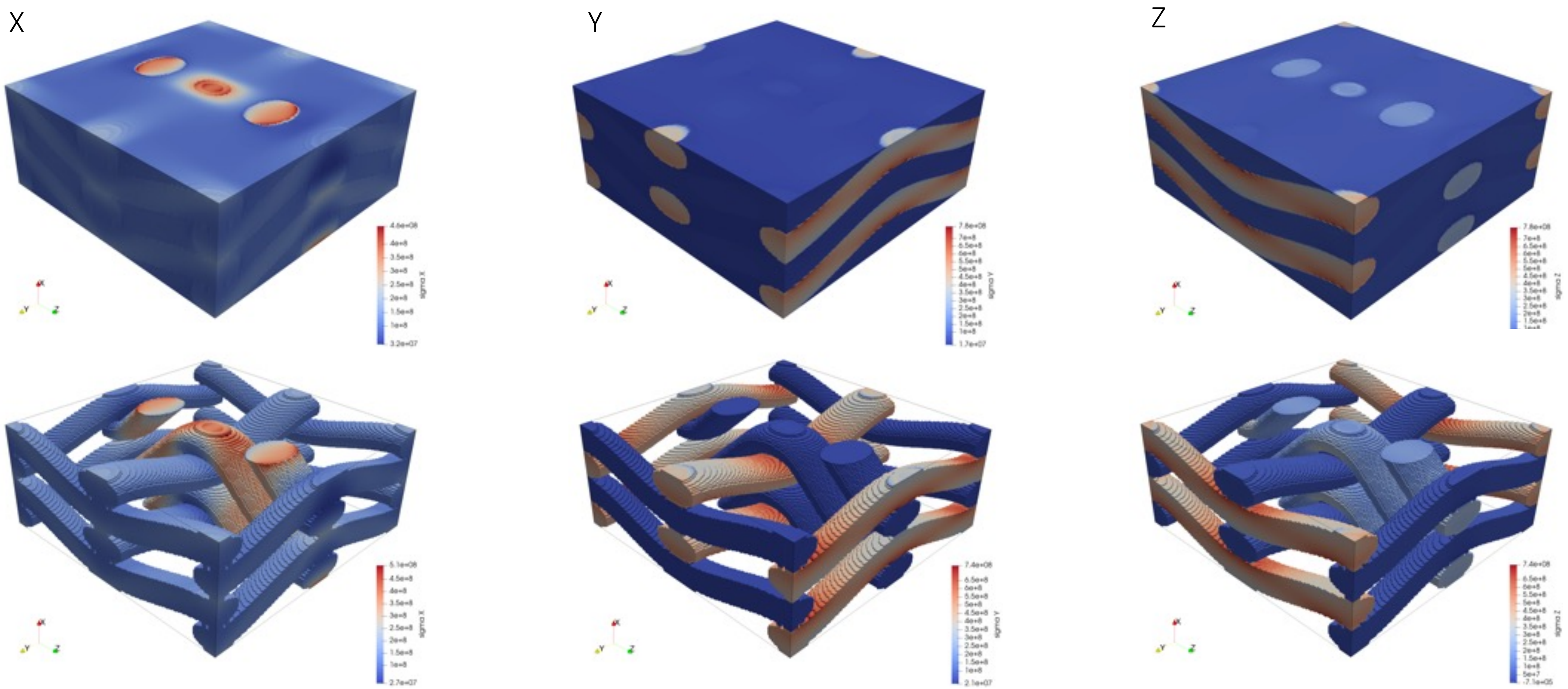

Fig.19 – Direct stress field with matrix visible (top) and matrix hidden (bottom) in the X, Y and Z directions

Unit Cell: Artificially Generated – Elasticity

Directions:
- X = 1
- Y = 2
- Z = 3

- The same methodology used at the micro-scale for the constituents was applied to obtain the effective mechanical properties of the unit cell.

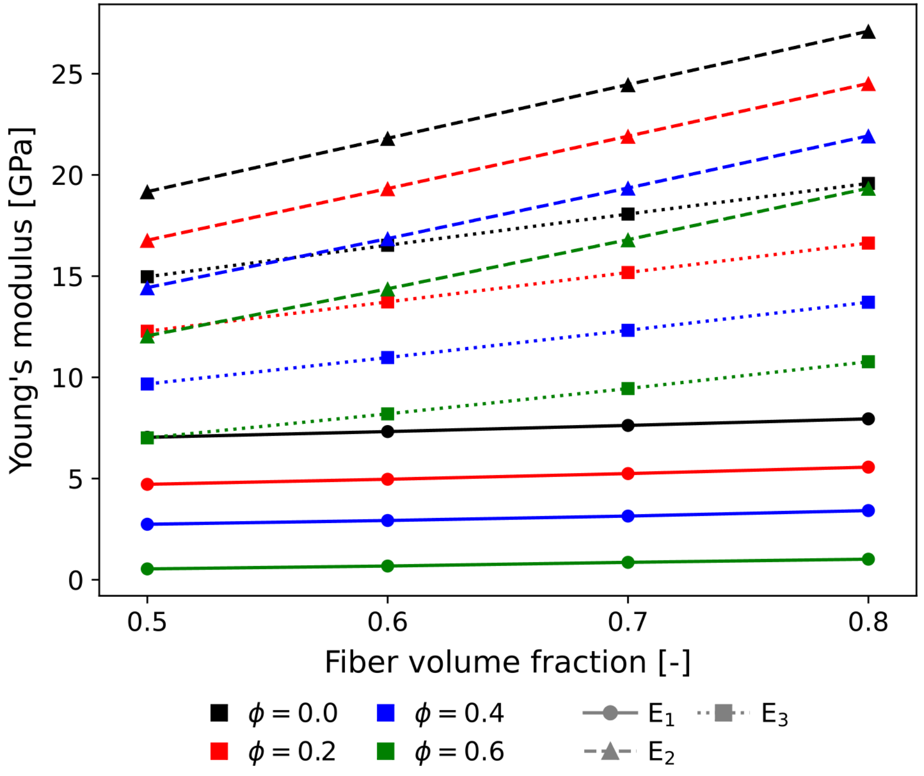

Young's moduli of the unit cell

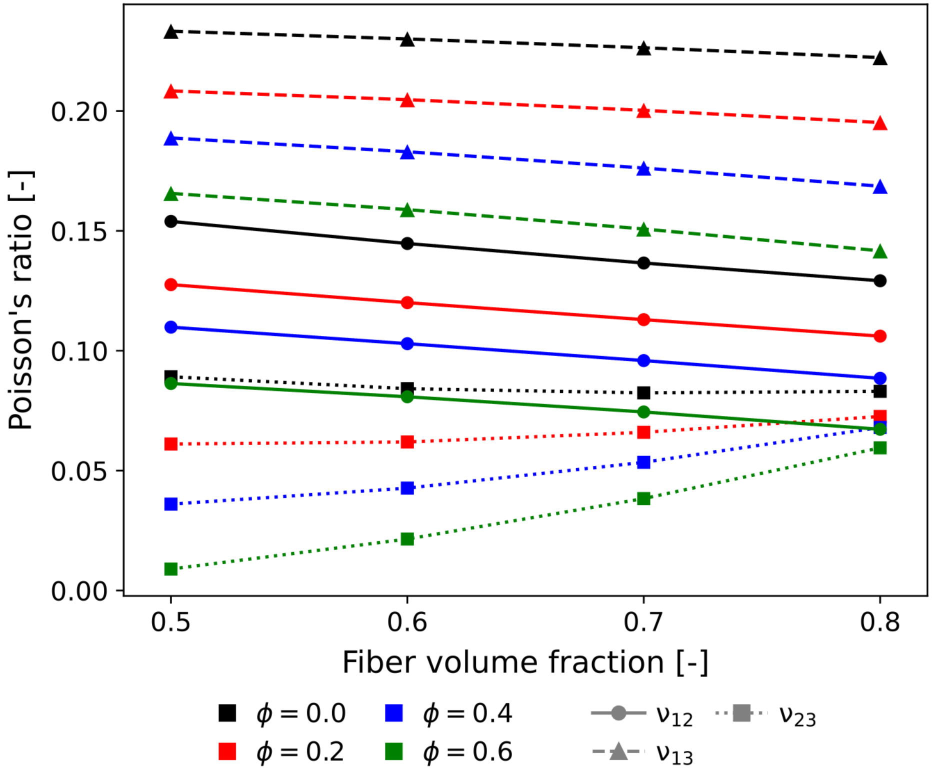

Poisson's ratios of the unit cell

Conclusions

- This work described a methodology to carry out multi-scale analyses of porous 3D woven materials using artificially generated models, and models segmented from microscopy / micro-CT data.
- This methodology can be applied to any type of composite material to obtain its homogenized orthotropic mechanical properties, and anisotropic thermal conductivity.
- The PuMA software allowed us to analyze the constituents at the micro-scale and then use those results to accurately model the unit cell at the macro-scale.
- Results were validated for the elasticity results of the porous matrix and the yarns by comparing them to analytical expressions listed in the literature.
- Future work investigate as-manufactured weaves.

Computational Materials Modeling

Increased Structural Refinement

Particle-based, discrete-element methods (LAMMPS, HYDRA)

Fiber-level resolution

Andrew P. Santos

Porous Microstructure Analysis (PuMA)

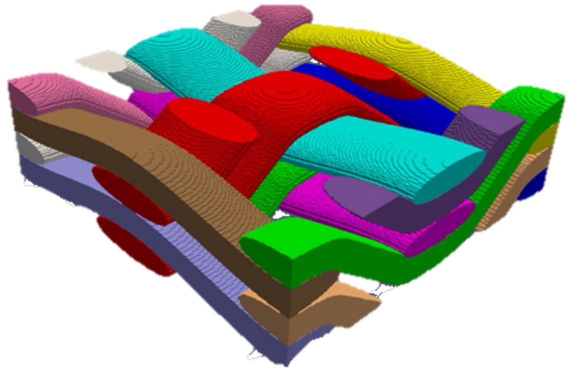

Yarn-level resolution

Sergio Friale Izquierdo

Increased Scale and Analysis

Particle-based/Meshless/Lagrangian Woven TPS Modeling

Goal of the bottom-up approach

- if the fiber model is correct, the weave will be correct
- extract fiber-level behavior and contribution in weaves and yarns during damage, impact or ablation

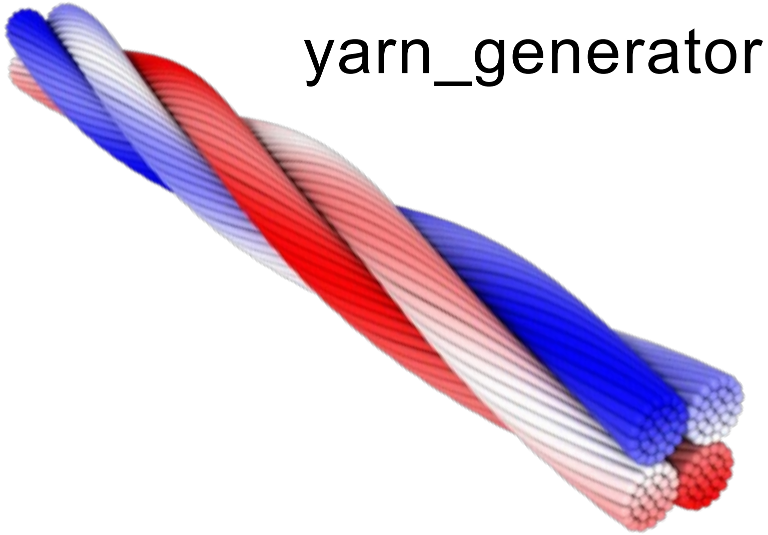

yarn_generator

Molecular dynamics

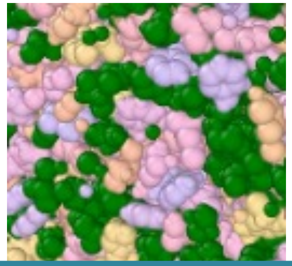

Explicit-fiber

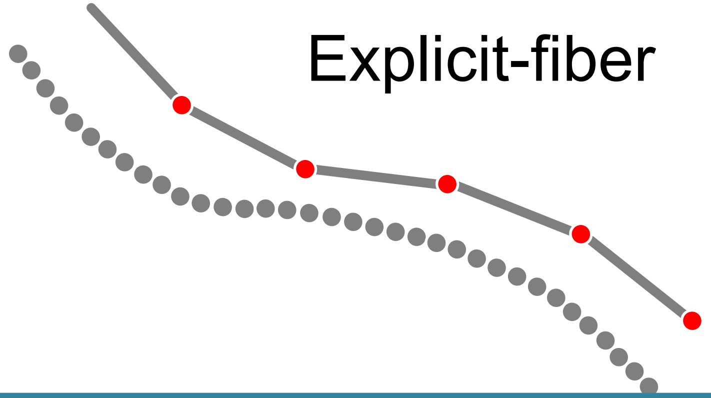

peridynamics

microscale

mesoscale

Phenomena Captured by Explicit-Fiber Modeling

Explicit-fiber modeling captures certain experimental observations where continuum is unable

<u>Physics incorporated with explicit-fiber models</u>

- Role of geometry and directionality
- Fiber-fiber friction
- Rupture
- Dynamic collective motion

<u>Explicit-fiber applications</u>

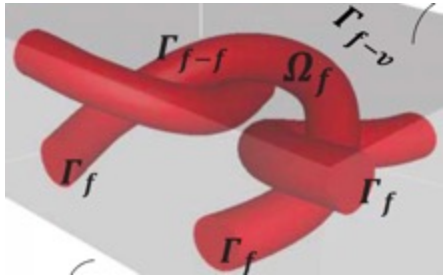

Strength of knit vs purl*

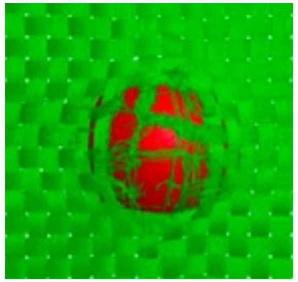

Impact with friction^

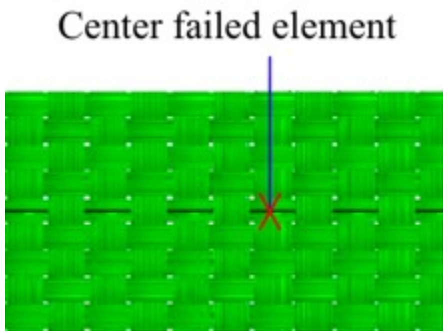

Friction controlled deformation with localized failure [+]

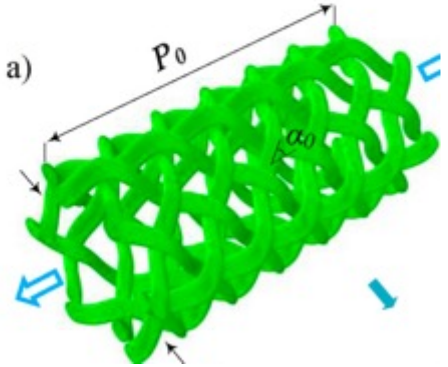

Yarn evolution during Braiding [#]

*Liu, D. *et al*. *J. App. Mech.* **2019**, *86* (11). doi.org/10.1115/1.4044014
[#]Ghaedsharaf, M. *et al*. *Composites Part B* **2021**, *218*, 108938. doi.org/10.1016/j.compositesb.2021.108938
[+]Wang, Y. *et al*. *Int. J. Impact Eng.* **2016**, *97*, 66–78. doi.org/10.1016/j.ijimpeng.2016.06.007
^Wang, Y.; *et al*. *Int. J. Impact Eng* **2016**, *97*, 66–78. doi.org/10.1016/j.ijimpeng.2016.06.007

Configuration Generation with Relevant Features

- Idealized and realistic yarn and weave configurations are required to calibrate and verify fiber models and test hypotheses on weaves
- Python package, yarn_generator, developed to generate fiber-level models of yarns and weaves

Two ways to generate a weave

Define or vary yarn paths

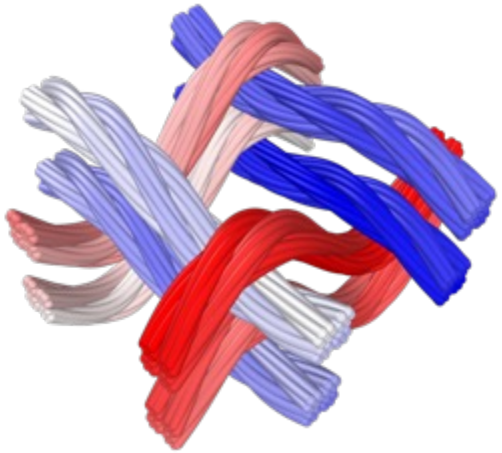

Yarn paths from CT

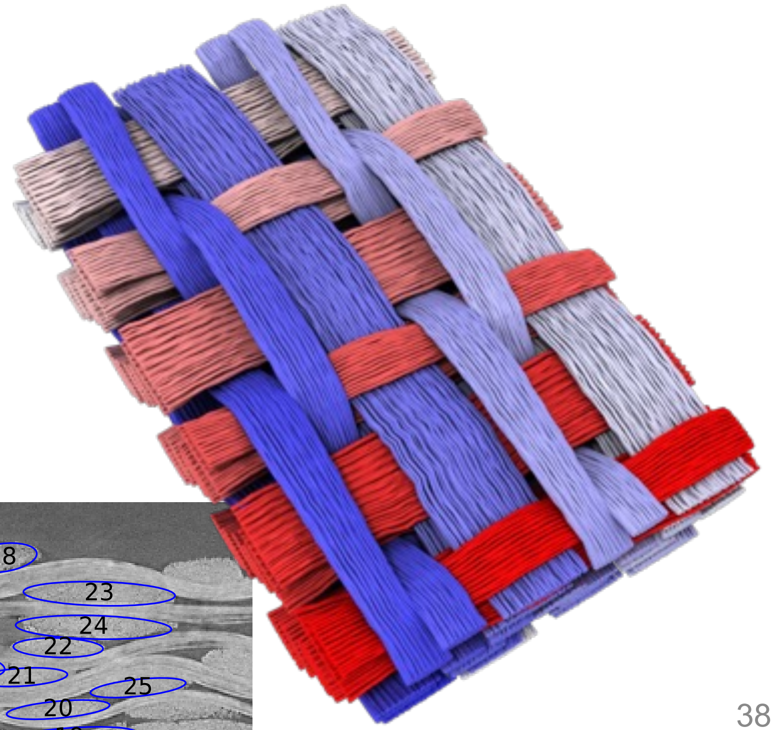

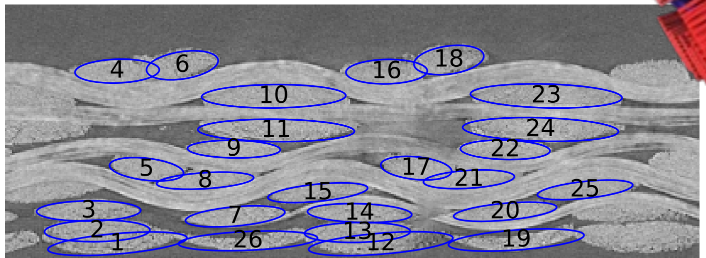

Yarn Features

Circular or ellipsoidal
cross sections

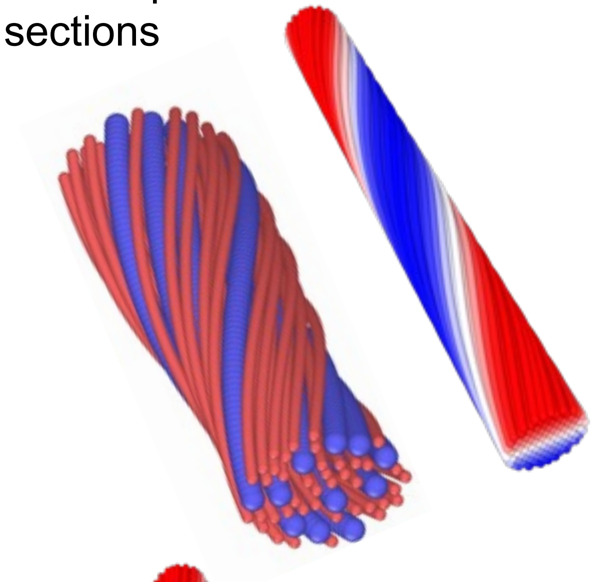

- Woven heat shields use yarns composed of different fibers and processing conditions
- Explicit-fiber simulations model the yarn microstructure
- The yarn_generator builds configurations with the relevant features

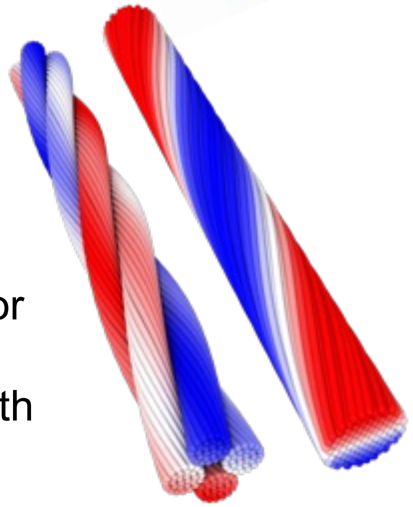

Single- or
multi-ply
yarns with
twisting

optimal circle-in-circle or
random 2d blended packing

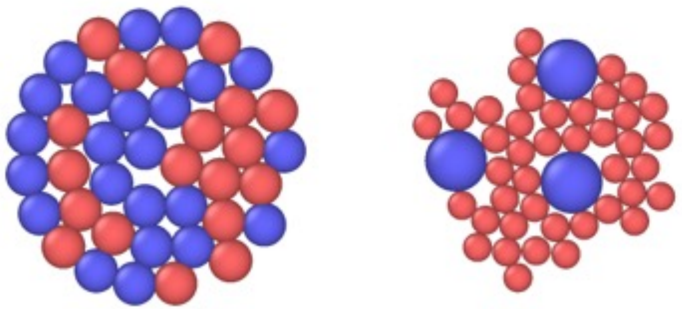

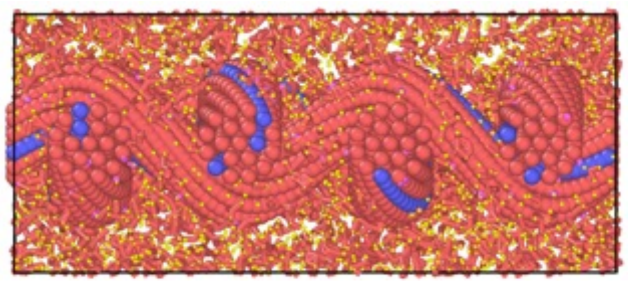

infusion

Yarn-Weave Manipulation

- Yarn manipulation can control the weave density or yarn packing
- Enables wrinkle and other behaviors
- Satisfies contact mechanics

circular packing protocol

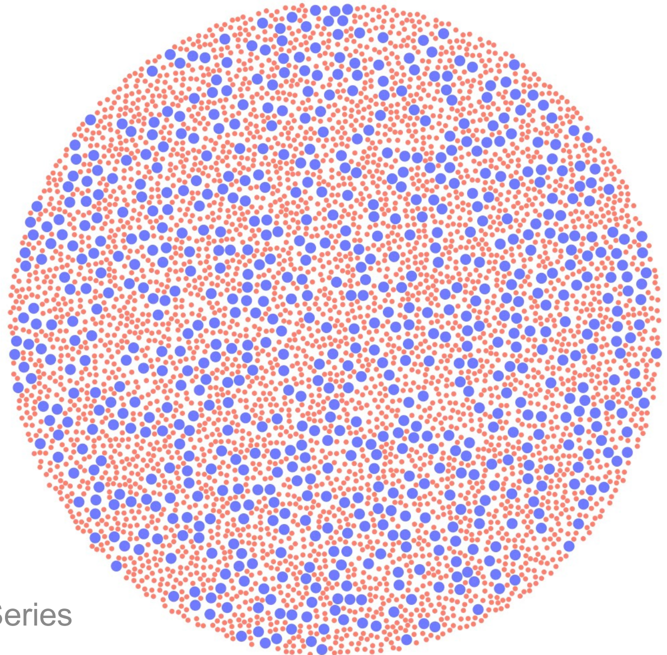

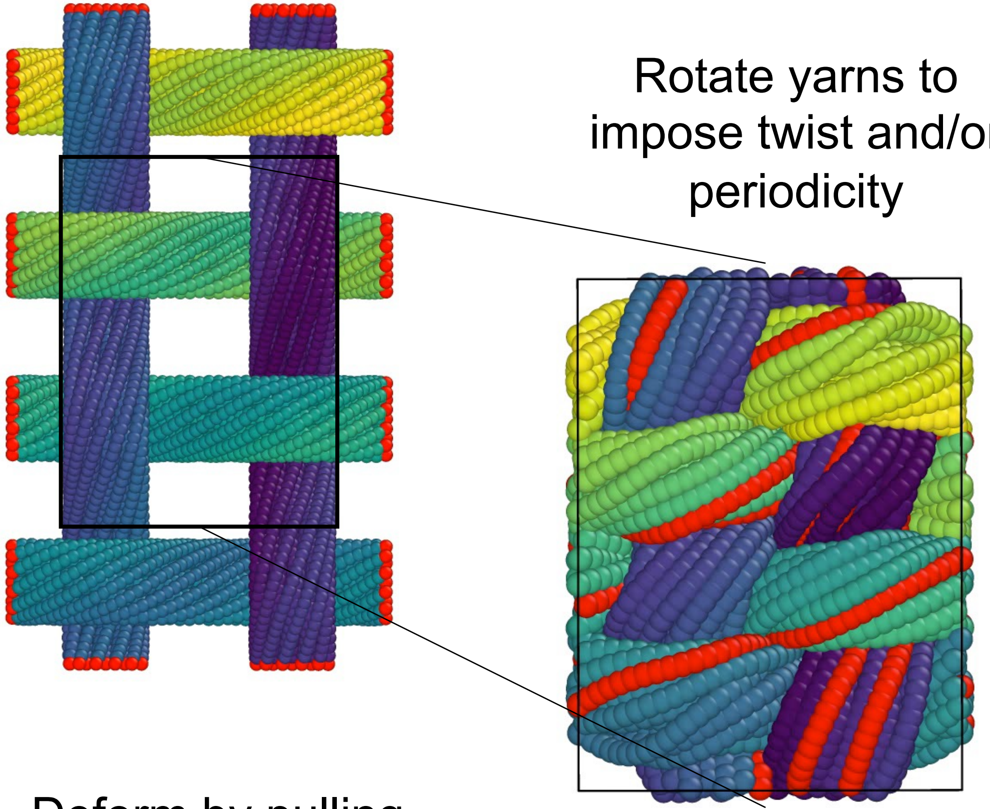

Rotate yarns to impose twist and/or periodicity

Deform by pulling yarn ends

Explicit-Fiber Simulation Methodology

Explicit-fiber simulations allow for the fibers to evolve independently during yarn-weave manipulation, parameterization and entry phenomena

yarn_generator

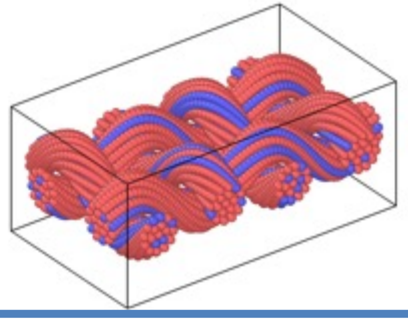

LAMMPS

Parameterization
Pull, Twist relaxation, 3-point bend, Thermal heating

micromechanics

Overlap contact forces
Friction, cohesion, viscoelasticity, conduction

Bonded forces
Stretch, bend, twist, rupture, conduction

Processes
Deformation, Ablation

Measurement
Moduli, Conductivity

Plimpton, S. J. et al., LAMMPS … . *Comp. Phys. Comm.* **2022**, *271*, 108171

Fiber Model Details

- Explicit-fiber simulation forces model each contact and internal mode independently
- Analysis of trajectories and forces can highlight the magnitude and directionality of each mode's contribution

Micromechanics-informed model:

- Intra[1,2]-fiber, bonded forces
  - Stretch
  - Bend
  - Shear
  - Twist
  - Rupture
- Inter[3]-fiber, contact forces
  - Friction
  - Viscoelastic repulsion
  - Cohesion

Method

- Meshless
- dynamic
- apply heat and deformation
- microstructure can change during simulation
- implemented in an open-source parallelized code[4]

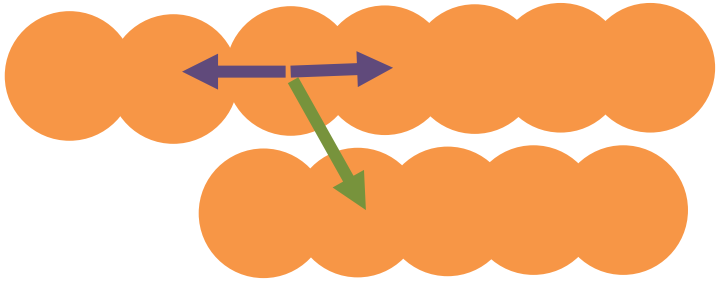

Most model forces are modeled as a Hookean spring + damping

$$f_r = k_r(r - r_0)$$

[1]Chen, X. et al. Comparative Assessment and Unification of Bond Models in DEM Simulations. *Granular Matter* **2021**, *24* (1), 29.
[2]Wang, Y. and Sun, X. Digital-Element Simulation of Textile Processes. *Composites Sci. Tech.* **2001**, *61* (2), 311–319.
[3]Silbert, L. E. et al., Granular Flow down an Inclined Plane: Bagnold Scaling and Rheology. *Phys. Rev. E* **2001**, *64* (5), 051302.
[4]Plimpton, S. J. et al., LAMMPS … . *Comp. Phys. Comm.* **2022**, *271*, 108171

Tensile, Bending and Shear Moduli

Tuning model spring parameters can capture the rupture behavior due to different modes for carbon fibers, *e.g.*, enabling experimental comparison

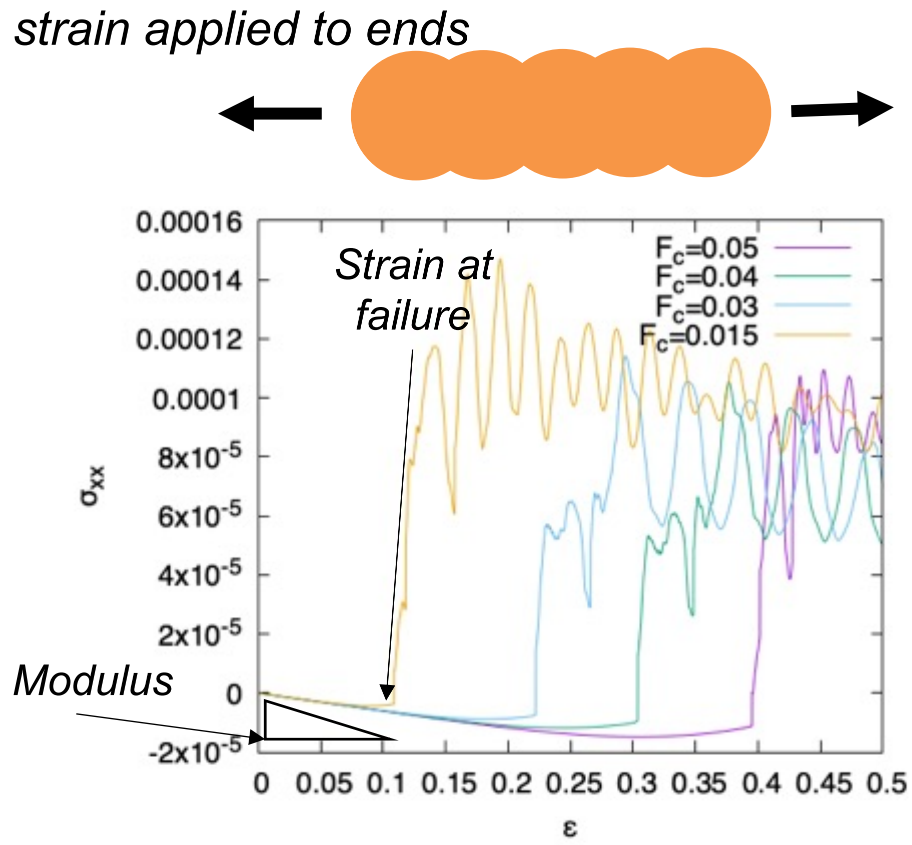

single, short fiber simulations

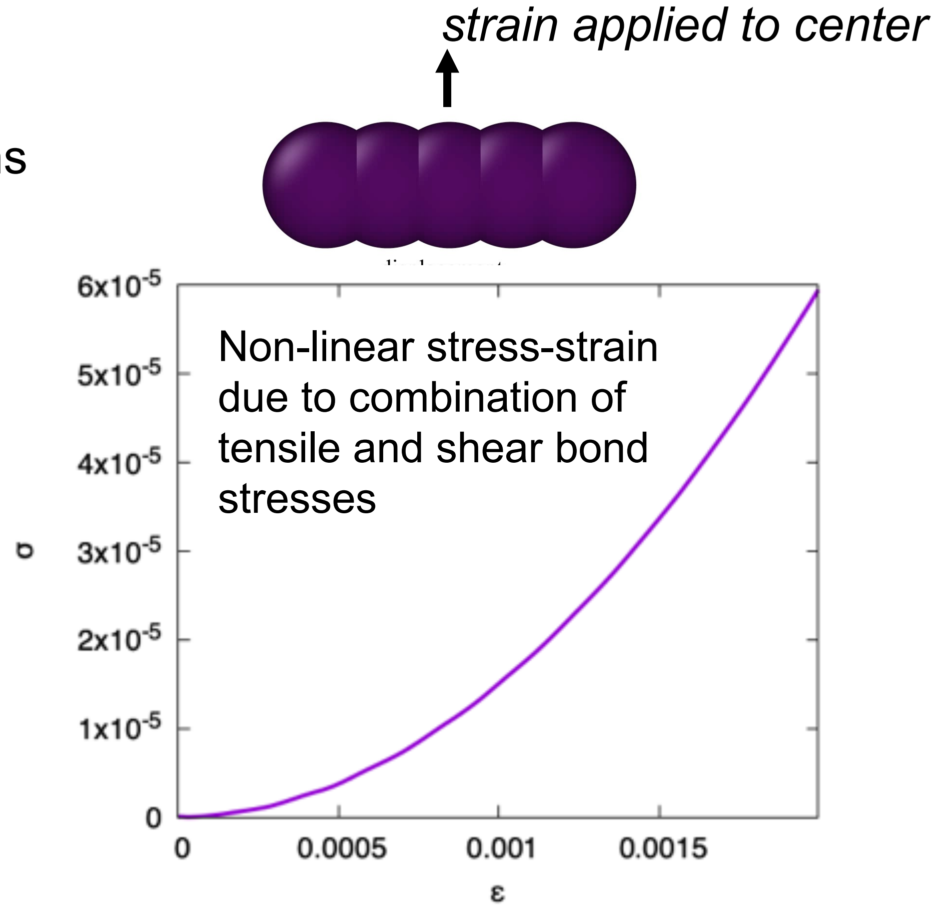

Rod Thermal Conduction Model

- Explicit-fiber models can characterize conduction along and across fibers
- New model enables thermo-mechanical processes
- Yarn feature-property relationships can be tested

7 twisted Kynol phenolic fibers

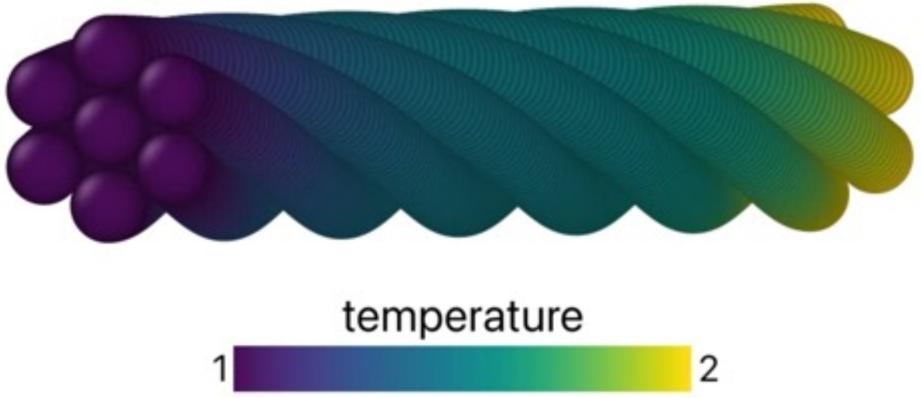

- Yarn coarse-graining changes the conduction timescale to steady-state due to
  - Number of fibers changes the contact area
  - Exterior fibers are longer than interior fibers in twisted yarns

- Strain slows approach to steady-state

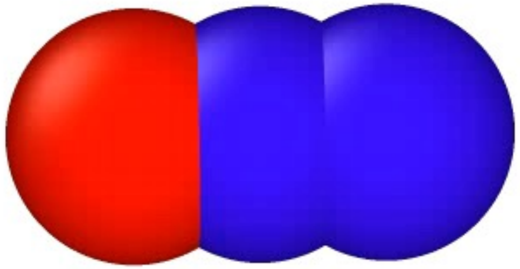

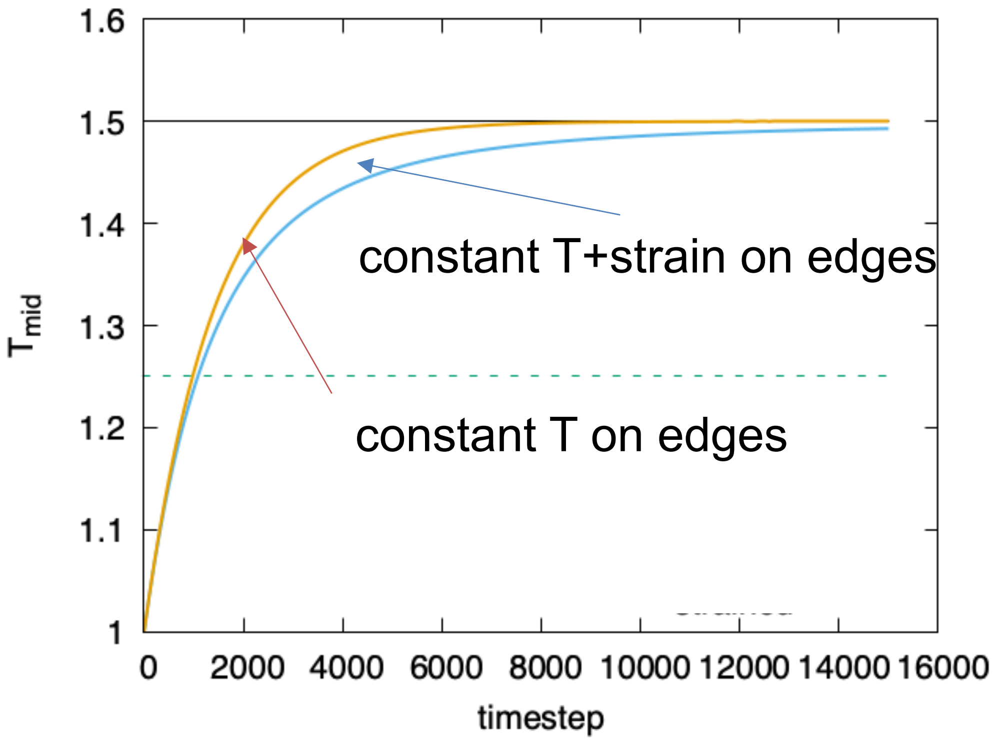

Weave Simulations of Heat Shield Ablation

The multi-fiber yarn representation can be incorporated into a full weave

Yarn

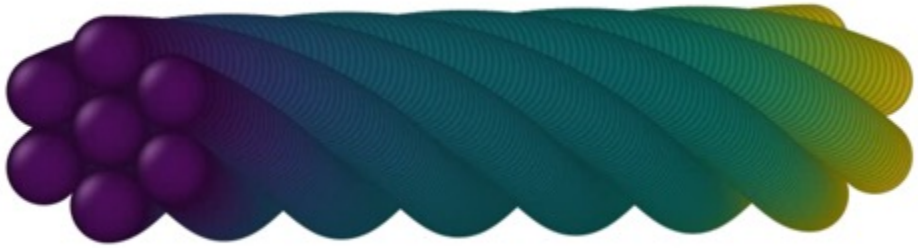

Periodic weave unit cell

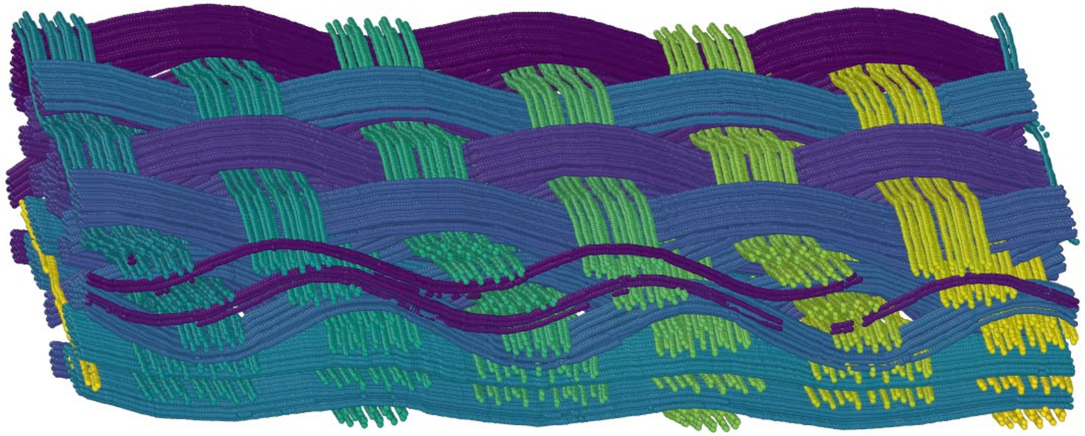

We can apply weave simulations to test hypotheses, such as heat shield ablation

State of Ablation Modeling

- Available ablation model (FIAT) shows that the standard approach to ablation (chemical only) underpredicts experimental recession values

- Ablation augmentation factor (AF) was proposed to scale chemical ablation rate to fit experiments:

$$\frac{\partial m}{\partial t} = (1 + AF)\frac{\partial m_c}{\partial t}$$

- The AF is not well posed but does appear to correlate to available surface shear stresses in some cases

- What are the contributing factors to non-chemical ablation augmentation?

ADEPT Weave

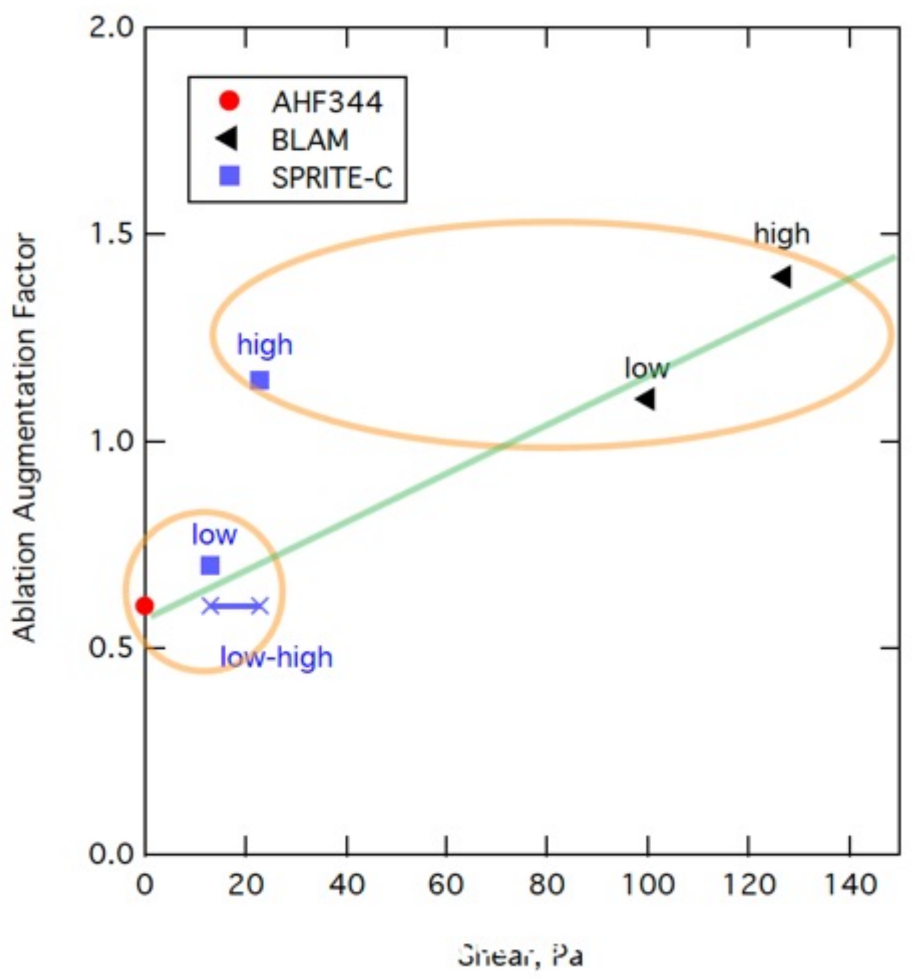

Courtesy F. Milos

Ablative Disconnection of Yarns

- Erosion of the weave such that regions of tows become disconnected and "fall off" from having no structural connection to the remaining weave

ADEPT Weave

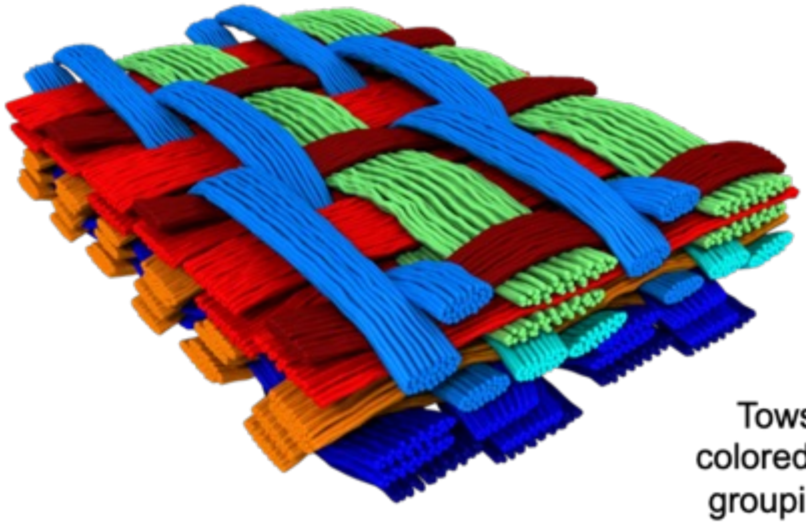

Tows colored by grouping

Weave before ablation

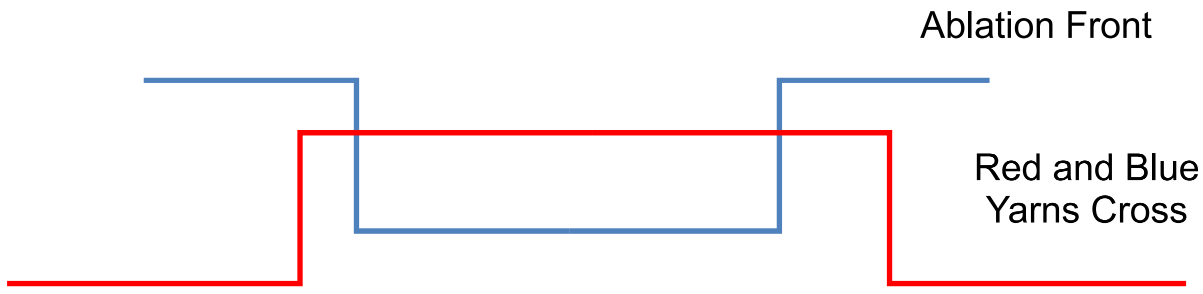

Weave at some point during ablation

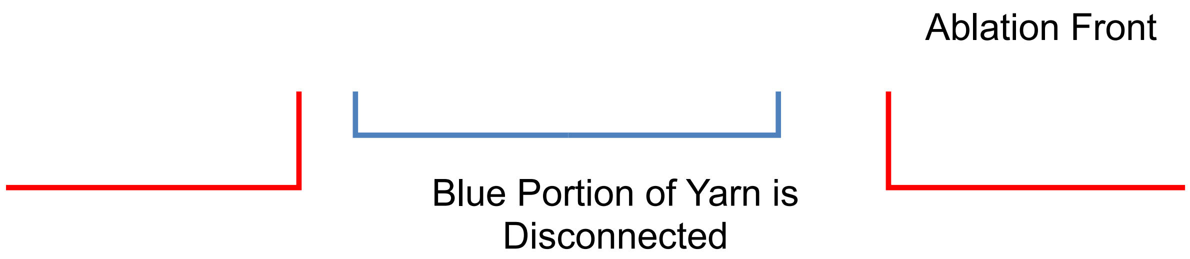

Model of Weave Ablation and Connectivity

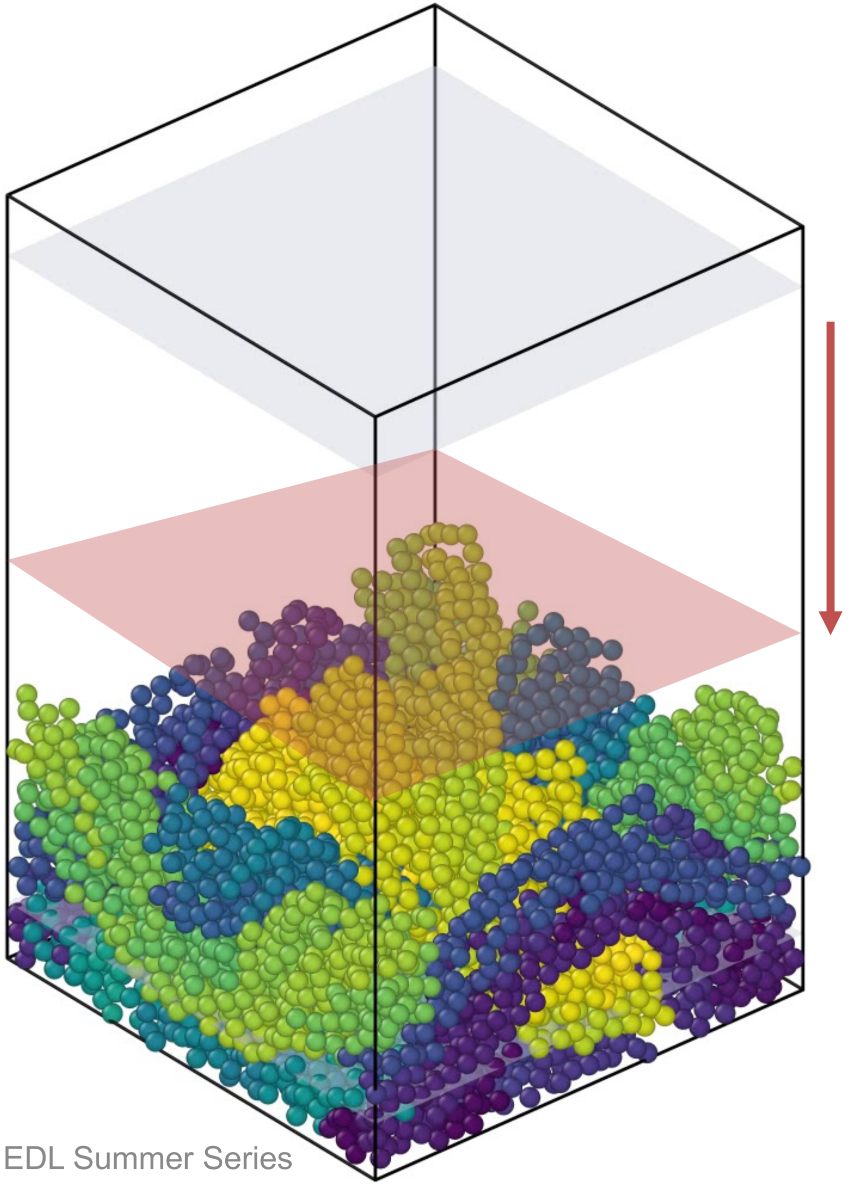

- Ablation front moves into the material and removes particles
- Forces applied such that disconnected portions of fibers are ejected from the surface into the ablation zone

ablation zone

Fiber tension: harmonic bonds
Fiber-fiber repulsion: viscoelasticity

Augmentation from Loss of Weave Connectivity

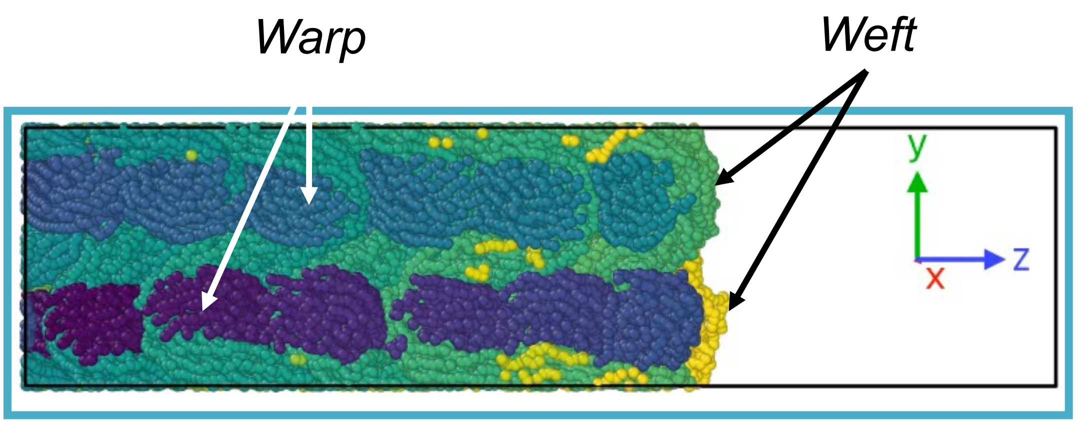

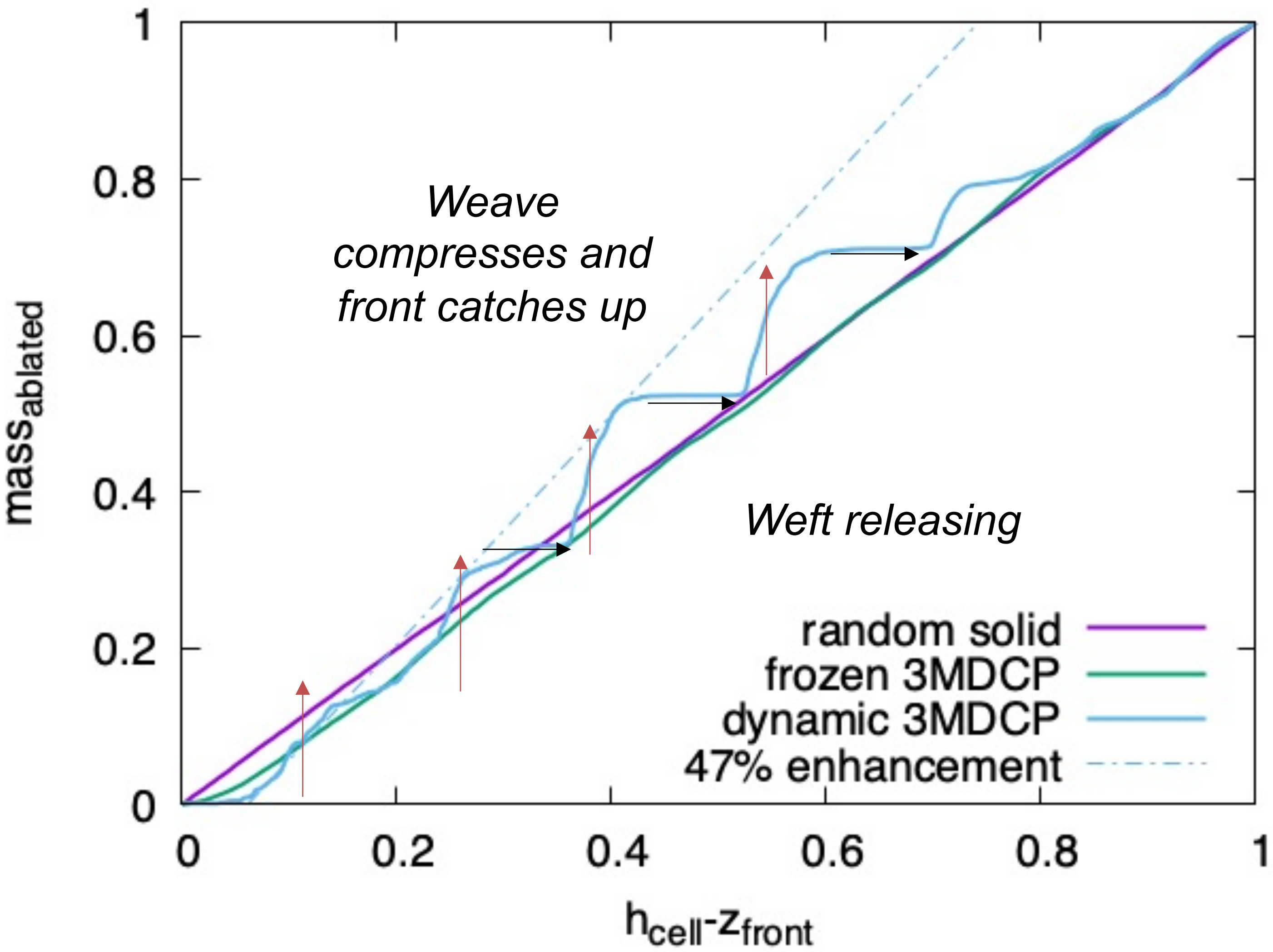

- Large portions of weft yarns ablate faster due to the 3D geometry
- Weave disconnection enhances erosion by ~47%
- Other phenomena, such as pitting, are likely present
- With more development, the method could predict this behavior

Explicit-Fiber Simulation Conclusions

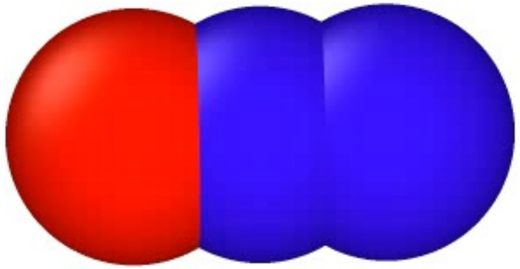

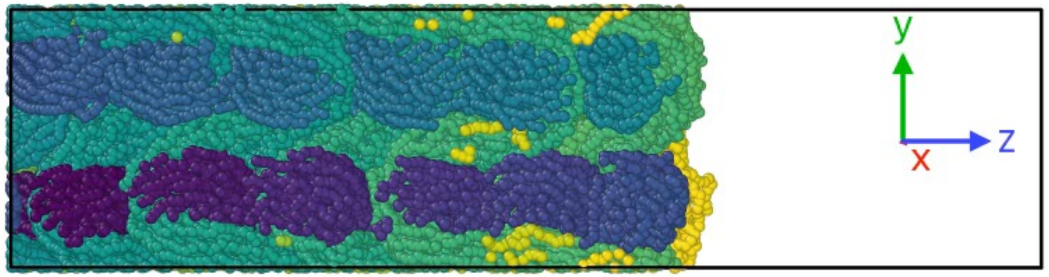

- Yarn processing, like twist, changes material properties, requiring explicit-fiber simulations
- Enabled modeling of thermo-mechanical behavior
- 3D woven heat shields have enhanced ablation, ~47%, due to the weave geometry

<u>Future work</u>

- Incorporate material-specific, coarse-grained yarn-models into full weaves
- Identify defect deformation mechanisms

Fiber and Weave Modeling Conclusions

- Entry System Modeling - Certification by Analysis task is
  - **Multi-center** (ARC-TSM, ARC-TI and GRC) and
  - **Multi-method** (non-destructive evaluation, machine learning, material characterization, finite element, peridynamics, explicit-fiber)
- The PuMA software
  - Measured the orthotropic mechanical properties, and anisotropic thermal conductivity
  - Modeled a composite woven system, and it's constituents, including the porous matrix and yarns
- Explicit-fiber simulations
  - Demonstrated a ~47% ablation enhancement due to the weave geometry

Porous Microstructure Analysis (PuMA)

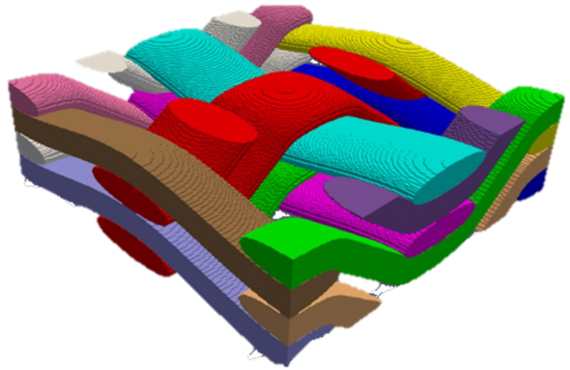

Particle-based, discrete-element methods (LAMMPS, HYDRA)